Since January 2020 Elsevier has created a COVID-19 resource centre with free information in English and Mandarin on the novel coronavirus COVID-19. The COVID-19 resource centre is hosted on Elsevier Connect, the company's public news and information website.

Methods 201 (2022) 49–64

Contents lists available at ScienceDirect

Methods

journal homepage: www.elsevier.com/locate/ymeth

Ultrasensitive detection and quantification of viral nucleic acids with Raindance droplet digital PCR (ddPCR)

Samuel Long *, Brian Berkemeier

AIDS and Cancer Virus Program, Frederick National Laboratory for Cancer Research, Frederick, MD 21702, United States

ARTICLE INFO

Keywords:
ddPCR
RT-ddPCR
SIV
HIV
Raindance
Inhibition
Viral reservoir
Cure research

ABSTRACT

Sensitive detection of viral nucleic acids is critically important for diagnosis and monitoring of the progression of infectious diseases such as those caused by SARS-CoV2, HIV-1, and other viruses. In HIV-1 infection cases, assessing the efficacy of treatment interventions that are superimposed on combination antiretroviral therapy (cART) has benefited tremendously from the development of sensitive HIV-1 DNA and RNA quantitation assays. Simian immunodeficiency virus (SIV) infection of Rhesus macaques is similar in many key aspects to human HIV-1 infection and consequently this non-human primate (NHP) model has and continues to prove instrumental in evaluating HIV prevention, treatment and eradication approaches. Cell and tissue associated HIV-1 viral nucleic acids have been found to serve as useful predictors of disease outcome and indicators of treatment efficacy, highlighting the value of and the need for sensitive detection of viruses in cells/tissues from infected individuals or animal models. However, viral nucleic acid detection and quantitation in such sample sources can often be complicated by high nucleic acid input (that is required to detect ultralow level viruses in, for example, cure research) or inhibitors, leading to reduced detection sensitivity and under-quantification, and confounded result interpretation. Here, we present a step-by-step procedure to quantitatively recover cell/tissue associated viral DNA and RNA, using SIV-infected Rhesus macaque cells and tissues as model systems, and subsequently quantify the viral DNA and RNA with an ultrasensitive SIV droplet digital PCR (ddPCR) assay and reverse transcription ddPCR (RT-ddPCR) assay, respectively, on the Raindance ddPCR platform. The procedure can be readily adapted for a broad range of applications where highly sensitive nucleic acid detection and quantitation are required.

1. Introduction

Sensitive detection of viral nucleic acids by PCR provides important prognostic and diagnostic information and is critical for monitoring the efficacy of treatment in infectious diseases such as those caused by SARS-CoV2, HIV-1 and other viruses [1–10]. Quantitative PCR (qPCR, also termed real-time PCR) derives the quantity of an analyte (i.e. pathogen nucleic acid) by comparing the threshold cycle (Ct) value, which is the PCR cycle at which fluorescence intensity reaches a preset threshold, with a standard curve generated from a series of samples of known target quantities, whereas digital PCR (dPCR) takes a different approach to measure target DNA molecule number in a sample. With dPCR, each reaction mixture is divided into thousands to millions of individual PCR reactions, depending on the dPCR platform. Partitioning occurs such that ideally, each reaction compartment contains at most one target molecule. These reactions are PCR amplified to the endpoint, the numbers of positive and negative reactions are counted, and the target copy number in the original sample is calculated. For samples with more concentrated targets, a given partition may contain two or more target molecules, in which case Poisson statistics modeling random

Abbreviations: BCP, 1-bromo-3-chloropropane; caDNA, cell-associated DNA; caRNA, cell-associated RNA; cART, combination antiretroviral therapy; CNV, copy number variation; Ct, threshold cycle; CV, coefficient of variation; ddPCR, droplet digital PCR; dPCR, digital PCR; GMO, genetically modified organism; HIV-1, human immunodeficiency virus 1; ICS, instrument control software; LoD, limit of detection; MGB, minor groove binder; miRNA, microRNA; M−MLV, Moloney Murine Leukemia Virus Reverse Transcriptase; NGS, next generation sequencing; NHP, non-human primate; PMT, photomultiplier tube; QC, quality control; qPCR, quantitative (real time) PCR; qRT-PCR, quantitative reverse transcription PCR; RT-ddPCR, reverse transcription droplet digital PCR; SARS-CoV2, severe acute respiratory syndrome coronavirus 2; SD, standard deviation; SIV, simian immunodeficiency virus; SSIII, SuperScript III reverse transcriptase; SSIV, SuperScript IV reverse transcriptase.

* Corresponding author.
E-mail address: Samuel.Long@nih.gov (S. Long).

https://doi.org/10.1016/j.ymeth.2021.04.025
Received 8 February 2021; Received in revised form 22 April 2021; Accepted 29 April 2021
Available online 3 May 2021

distribution of DNA templates into the compartments is used to accurately calculate the target molecule quantity in the starting sample. The ability for direct absolute quantitation without the need for calibration curves is particularly important for analytes for which well-characterized reference material is not readily available. Additional advantages of dPCR include higher quantitation precision as indicated by improved coefficients of variation (CVs) relative to those of qPCR assays, less susceptibility to inefficient amplification which can occur due to PCR inhibitors or primer mismatches, as well as the potential for measuring a large number of different targets in the same reaction due to dPCR's unique capability of amplitude or ratio-based higher order multiplexing [11–13].

dPCR has been utilized in increasingly more and broader fields such as rare allele/mutation detection [14–18], genetically modified organism (GMO) screening [19], pathogen detection (including SARS-CoV 2) [20–33], gene and miRNA expression analysis [34,35], copy number variation (CNV) determination [36,37], as well as absolute quantification of reference material, standards and NGS libraries [38]. The technique has especially been useful in detecting and quantifying many types of viruses, among which HIV measurement constitutes the largest fraction of applications (reviewed in [39]). The technology has also gained utility in SARS-CoV-2 detection, and shown to have superior sensitivity compared to quantitative reverse transcription PCR (qRT-PCR), as highlighted by several recent studies [40–42].

From the platform performance perspective, dPCR traditionally has been perceived to present two main limitations. (1) The most commonly used dPCR platforms generally allow a relatively small total nucleic acid input in each reaction. For example, the 60 ng to 1 μg upper limit on DNA template input allowed on some platforms correspond to ~ 9000 and ~ 150,000 mammalian genome-equivalent of cellular DNA respectively. A previous study [43] suggested that sensitivity limitations of dPCR systems are mainly determined by how much template DNA can be accommodated in each reaction. (2) The second commonly perceived disadvantage of dPCR associated with some established platforms is limited dynamic range. The dynamic range of dPCR by definition is determined by the number of partitions that are available for each sample. For example, most dPCR platforms partition each sample to 3000–40000 individual partitions. The limited dynamic range of these platforms consequently requires dilutions of many input samples to achieve accurate measurements [44]. The current protocol, which was developed based on the Raindance ddPCR platform, aims to address these two limitations. We recently demonstrated [20] that on this platform, at least 8 million mammalian cell equivalent genomic DNA (~53 μg) could be included in each reaction without compromising the droplets' integrity or quantity during the dropletization step (based on the QC droplet results during dropletization). In addition, each reaction can tolerate up to 4 million mammalian cell equivalent of genomic DNA without introducing inhibition during the quantification of a viral target. The Raindance ddPCR platform, therefore, drastically increases the input DNA template quantity that can be accommodated in each reaction. This platform also offers significantly expanded dynamic range (i.e. 6 log) by increasing the partition number for each sample to 10 million droplets. This quantification dynamic range approaches or is comparable to that which is achieved in qPCR systems.

The current protocol was developed for ultrasensitive analysis of the nucleic acids of the simian immunodeficiency virus (SIV), a HIV-1 model using the nonhuman primate (NHP) animal system for infection, pathogenesis and cure research [7,45–52]. SIV-infected Rhesus macaques captures many key aspects of human HIV patients including the persistence of a latent viral reservoir in resting memory CD4 + T cells even after prolonged combinatorial antiretroviral therapy (cART). As cell and tissue associated HIV-1 DNA (caDNA) and RNA (caRNA) (as opposed to plasma viral load) have emerged as strong predictors of viral rebound and disease progression after cART treatment interruption [10,53], accurate and sensitive measurement of nucleic acids from these samples from infected animals subjected to treatment regimens becomes especially important in determining which interventions are successful in decreasing the latent reservoir size, and should be given priority. The amount of total nucleic acid in a sample that can be analyzed in each PCR reaction is an important contributing factor to the overall assay sensitivity. Ultrasensitive detection of viral DNA often requires a sample input amount that exceeds the capacity of each qPCR or dPCR reaction (e.g. BioRad ddPCR). For example, even with an assay that has been optimized to be able to detect every target signal that is present, i.e. a single copy detection assay with the most sensitive limit of detection (LoD) of 3 copies per PCR reaction, to reliably detect (i.e. at 95% confidence) the viral signal at the level of 1 copy of viral DNA in 1 million cells, at least 3 million mammalian cell equivalent DNA (~20 μg) needs to be analyzed, assuming Poisson distribution of target molecules. Exceeding the per reaction input capacity of these platforms often leads to significant reaction inhibition during quantification, likely due to a combination of the DNA template quantity and copurifying inhibitors from tissues [54]. Some qPCR and dPCR methods use multiple replicates to sidestep the sample input limit and associated inhibitor issues through diluting or splitting samples until there is no obvious inhibition. Significant effort may therefore be required to identify the optimal (defined as maximal input without inhibition) per-reaction input for each individual sample using this approach. In comparison, due to its capacity for a large quantity of DNA input in each reaction, and the ability to overcome inhibition [20], the Raindance platform allows quantitation of ultralow viral target DNA from a large background of DNA derived from cell or tissue sources. In the current protocol we also describe the use of a high processivity reverse transcriptase combined with the Raindance ddPCR platform for detection of SIV RNA. This combination was previously shown to be able to overcome severe quantitation inhibition in RNA samples extracted from Rhesus macaque tissues to enable ultrasensitive SIV detection [20]. With proper modifications and adaptations, this protocol can be generalized and used for analysis of other viruses or targets from animal cell and tissue sources.

2. Materials

2.1. Method overview

The overall protocol consists of five parts, among which protocols 3.1, 3.4 and 3.5 apply to viral DNA quantitation, and protocols 3.2, 3.3, 3.4 and 3.5 apply to viral RNA quantitation:

Protocol 3.1 Quantitative recovery of DNA from cells and animal tissues. In this part of the protocol, DNA is back extracted from the interphase and phenol phase of cell or tissue homogenates made in TriReagent (Molecular Research Center), while the upper, aqueous phase is saved for isolating RNA (see Protocol 3.2). TriReagent is a monophase solution containing phenol and guanidine thiocyanate and provides a cost effective and efficient method of nucleic acid isolation. This is a precipitation-based method that allows nearly quantitative recovery of nucleic acids [55,56] from diverse sample types or tissues and enables maximizing the amount of nucleic acid input in downstream reactions and minimizes signal loss. This is especially beneficial when the starting material is limited. Other DNA isolation methods (such as column-based methods) can be considered for applications in which quantitative recovery of nucleic acids from sample sources is not critical. For further discussion on quantitative recovery of nucleic acids in viral detection, see [54].

Protocol 3.2 Quantitative recovery of RNA from cells and animal tissues. This is also precipitation-based. The procedure is effective for isolating intact RNA molecules of all types from 100 bases to 15 kilo bases in length.

Protocol 3.3 Reverse transcription. A high processivity reverse transcriptase, SuperScript IV (SSIV) is used in this part of the protocol. Alternatively, M−MLV reverse transcriptase or SuperScript III (SSIII) can be used.

Protocol 3.4 Raindance droplet digital PCR. In this part of the

protocol, sample DNA that is purified in Protocol 3.1 or cDNA generated in Protocol 3.3 is combined with assay primers, probe(s) and other components required for droplet generation and digital PCR reaction. This mixture is subject to dropletization (up to 10 million droplets generated per 50 μL reaction) on the Raindance Source instrument. The partitioned mixture then undergoes PCR thermal cycling, followed by fluorescence droplet detection on the Raindance Sense instrument.

Protocol 3.5 Data analysis and report generation. In this part of the protocol, the RainDrop Analyst II software is used to evaluate the raw sense (i.e. fcs) files generated after Protocol 3.4 to enable quantitation, statistical analysis and creation of final reports in graph and/or quantitative tabular format. The software incorporates standard statistics functions including mean, median, mode, CV, standard deviation (SD) and ratio (a function frequently used to determine the percentage of droplets that are positive or negative for a given assay, or the ratio of mutant vs. wild-type populations). The software also includes the Poisson correction function, which is especially important in cases where some droplets may contain more than one copy of the target molecule, and in applications where duplex assays or higher order multiplex reactions are employed [20].

2.2. Materials

In this section, the reagents, consumables, reagent recipes, and equipment for each protocol are listed separately, except for protocols 3.1 and 3.2, which share a significant number of reagents, consumables and equipment.

2.2.1. Reagents for DNA and RNA extraction and preparation

2.2.1.1. Shared. TriReagent (TR 118, Molecular Research Center, Cincinnati, OH)

1-bromo-3-chloropropane (BCP) (BP 151, Molecular Research Center, Cincinnati, OH)

Glycogen (34990920, Roche, Indianapolis, IN)

Isopropanol (I9516, Sigma-Aldrich, St. Louis, MO)

Ethanol (459836, Sigma-Aldrich, St. Louis, MO)

2.2.1.2. DNA specific. DNA Back Extraction Solution (GT 192, Molecular Research Center, Cincinnati, OH)

Tris pH 9.0 1 M (T2819, Sigma-Aldrich, St. Louis, MO)

2.2.1.3. RNA specific. Tris pH 8.0 1 M (T2694, Sigma-Aldrich, St. Louis, MO)

2.2.2. Consumables for DNA and RNA extraction and preparation

Tissue homogenizing CKMix – 2 mL (i.e. homogenization tubes containing ceramic (zirconium oxide) beads as grinding material, for 20 mg to 200 mg tissue quantity range) (P000918-LYSK0-A, Bertin Instruments, Montigny-le-Bretonneux, France)

(Optional) Tissue homogenizing CK28 – 7 mL (for 200 mg to 2 g tissue quantity range) (P000935-LYSK0-A, Bertin Instruments, Montigny-le-Bretonneux, France)

(Optional) Hard tissue homogenizing CK28 – 15 mL (for 400 mg to 4 g tissue quantity range) (P000947-LYSK0-A, Bertin Instruments, Montigny-le-Bretonneux, France).

2 mL microfuge tubes (i.e. that can resist high centrifugation forces up to 25,000 xg) (72.704.200, Sarstedt, Newton, NC)

(Optional) Eppendorf Tube 5.0 mL (i.e. that can resist high centrifugation forces up to 25,000 xg) (0030119460, Eppendorf AG, Hamburg, Germany)

2.2.3. Reagents for reverse transcription

MgCl2 25 mM (R0971, ThermoFisher Scientific, Waltham, MA)

dNTP (dATP, dCTP, dGTP, dTTP) mix, each nucleotide at a concentration of 25 mM (R1121, ThermoFisher Scientific, Waltham, MA)

DTT 0.1 M (707265ML, ThermoFisher Scientific, Waltham, MA)

Primer **SIVNestR01** (Table 1) (desalted) 100 μM (dissolved in 10 mM Tris pH 9.0) (IDT, Coralville, IA)

GeneAmp 10x PCR buffer II (N8080010, ThermoFisher Scientific, Waltham, MA)

Tween 20 (P9416, Sigma-Aldrich, St. Louis, MO)

RNaseOUT (Recombinant ribonuclease inhibitor) (10777019, ThermoFisher Scientific, Waltham, MA)

SuperScript IV (SSIV) reverse transcriptase (18090010, ThermoFisher Scientific, Waltham, MA)

(optional) M−MLV reverse transcriptase (28025013, ThermoFisher Scientific, Waltham, MA)

(optional) SuperScript III (SSIII) reverse transcriptase (18080093, ThermoFisher Scientific, Waltham, MA)

RNA extracted in protocol 3.2, or user-provided control sample(s) or reference standard

2.2.4. Reagents for ddPCR

Target (viral) assay forward primer: **SGag forward** (Table 1) (desalted) 100 μM (dissolved in 10 mM Tris pH 9.0) (LGC Biosearch Technologies, Hoddesdon, UK)

Target (viral) assay reverse primer: **SGag reverse** (Table 1) (desalted) 100 μM (dissolved in 10 mM Tris pH 9.0) (LGC Biosearch Technologies, Hoddesdon, UK)

Target (viral) assay MGB probe (labeled with FAM fluorophore): **SGag ddPCR probe** (Table 1) (4316034, ThermoFisher Scientific, Waltham, MA) 10 μM (dissolved in 10 mM Tris pH 9.0)

Reference assay forward primer: **RCCR5 forward** (Table 1) (desalted) 100 μM (dissolved in 10 mM Tris pH 9.0) (Coralville, IA)

Reference assay reverse primer: **RCCR5 reverse** (Table 1) (desalted) 100 μM (dissolved in 10 mM Tris pH 9.0) (Coralville, IA)

Reference assay MGB probe (labeled with VIC fluorophore): **RCCR5 ddPCR probe** (Table 1) (4316034, ThermoFisher Scientific, Waltham, MA) 10 μM (dissolved in 10 mM Tris pH 9.0)

TaqMan genotyping master mix (4371353, Thermofisher Scientific, Waltham, MA)

dNTP (dATP, dCTP, dGTP, dTTP) mix, each nucleotide at a concentration of 100 mM (10297018, ThermoFisher Scientific, Waltham, MA)

DNase and RNase free H2O (AM9932, ThermoFisher Scientific, Waltham, MA)

Droplet stabilizing buffer (p/n 30–06086, Bio-Rad, Hercules, CA)

Table 1
Sequences of primers and probes used in the reverse transcription and ddPCR steps.

Primer	Sequence	Note
SIVNestR01	GTTGGTCTACTTGTTTTTGGCATAGTTTC	
SGag forward	GTCTGCGTCAT(dP)TGGTGCATTC	dP [57] denotes a nonstandard base
SGag reverse	CACTAG(dK)TGTCTCTGCACTAT(dP)TGTTTTG	dK [57] and dP denote nonstandard bases
RCCR5 forward	CCAGAAGAGCTGCGACATCC	
RCCR5 reverse	GTTAAGGCTTTTACTCATCTCAGAAGCTAAC	
Probe	**Sequence**	
SGag ddPCR probe	5′-FAM- CTT CYT CAG TRT GTT TCA CTT T -MGB	
RCCR5 ddPCR probe	5′ VIC- TTC CCC TAC AAG AAA CT-MGB	

DNA extracted in protocol 3.1, or user-provided control sample(s) or reference standard

Or cDNA generated in protocol 3.3

2.2.5. Consumables for ddPCR

1.5 mL low binding micro tubes for DNA (72.706.700, Sarstedt, Newton, NC)

Raindance source chip (p/n 30–04295, Bio-Rad, Hercules, CA)

8-strip PCR tubes, 0.2 mL (PCR-0208-CP C, Axygen, Corning, NY)

RainDrop Elastomer (standard PCR) tube strip cap (p/n 40–06087, Bio-Rad, Hercules, CA)

RainDrop sense chip (p/n 30–04296, Bio-Rad, Hercules, CA)

High-speed PCR tube cap (p/n 40–08286, Bio-Rad, Hercules, CA)

2.3. Recipes

2.3.1. Reagent recipes for DNA extraction and preparation

10 mM pH 9.0 Tris solution: 1 M Tris pH 9.0 and DNase and RNase free H2O in 1:99 ratio (e.g. 1 mL 1 M Tris pH 9.0 + 99 mL H2O)

70% ethanol: ethanol and DNase and RNase free H2O in 70:30 (v/v) ratio (e.g. 70 mL ethanol + 30 mL H2O)

2.3.2. Reagent recipes for RNA extraction and preparation

10 mM pH 8.0 Tris solution: 1 M Tris pH 8.0 and DNase and RNase free H2O in 1:99 (v/v) ratio (e.g. 1 mL 1 M Tris pH 8.0 + 99 mL H2O)

70% ethanol: ethanol and DNase and RNase free H2O in 70:30 (v/v) ratio (e.g. 70 mL ethanol + 30 mL H2O)

2.3.3. Reagent recipe for reverse transcription

GeneAmp 10x PCR buffer II with 2% Tween 20: GeneAmp 10x PCR buffer II and Tween 20 in 98:2 (v/v) ratio (e.g. 98 mL GeneAmp 10x PCR buffer II + 2 mL Tween)

2.4. Equipment

2.4.1. Equipment for DNA and RNA extraction and preparation

2.4.1.1. Shared. Precellys Evolution tissue homogenizer (P000062-PEVO0-A, Bertin Instruments, Montigny-le-Bretonneux, France)

(Optional) 7 mL holder pack for Precellys Evolution (S000911-PEVO0-A, Bertin Instruments, Montigny-le-Bretonneux, France)

(Optional) 15 mL holder pack for Precellys Evolution (S000810-PEVO0-A, Bertin Instruments, Montigny-le-Bretonneux, France)

Sorvall Legend Micro 21R Microcentrifuge (75002445, Thermo Scientific, Waltham, MA)

(Optional) Eppendorf centrifuge 5430 with rotor FA-45–16-17 (5427750002, Eppendorf AG, Hamburg, Germany)

Vortex mixer (10153–688, VWR, Radnor, PA)

Nanodrop 2000/2000c spectrometer (ND-2000, ThermoFisher Scientific, Waltham, MA)

2.4.1.2. DNA specific. (Optional) Branson SFX150 Sonifier (SFX150, Emerson Industrial Automation, Danbury, CT)

2.4.2. Equipment for ddPCR

RainDrop Source instrument (20–04401, Bio-Rad, Hercules, CA)

C1000 Touch Thermal Cycler with 96-deep well reaction module (1851197, Bio-Rad, Hercules, CA) (Or an equivalent thermocycler that meets the following specifications: (a) block format should accommodate standard 0.2 mL tubes; (b) adjustable-height heated lid with the surface of the heated lid being hard and texture-free; (c) adjustable ramp speed.)

RainDrop Sense instrument (20–04402, Bio-Rad, Hercules, CA) (including a chip compression plate)

2.4.3. Equipment for data analysis and report generation

A workstation with Windows 7, 64-bit operating system, SP1 or greater (or Mac OS X) installed with RainDrop Analyst II software (Bio-Rad, Hercules, CA) and with the following minimum configurations: Java 8; Intel i7 processor or greater; 8 GB RAM or greater and at least 100 GB Hard disk space. The recommended display monitor for RainDrop Analyst II is 1920 × 1080 (landscape).

Note: RainDrop Analyst II will operate on Windows 7, 32-bit operating system with suboptimal performance and at lower resolution displays (down to 1024 × 768) with lower image quality.

Software: Raindance Analyst II (Bio-Rad, Hercules, CA)

3. Protocols

3.1. Quantitative recovery of DNA from cells and animal tissues

1. Cell pellets or tissue specimens of ≤ 200 mg each are collected in or transferred into 2 mL homogenization tubes containing ceramic (zirconium oxide) beads as grinding material. Add 1 mL TriReagent into each tube. Alternatively, tissue specimens of 200 mg to 2 g quantity range, or 400 mg to 4 g quantity range, are collected in or transferred into 7 mL or 15 mL homogenization tubes containing ceramic (zirconium oxide) beads as grinding material, respectively. Scale up the TriReagent amount accordingly if 7 mL or 15 mL homogenization tubes are used.

Note: Tissue samples larger than 4 g should be divided into smaller portions for processing so as not to exceed homogenization tube capacity.

2. Program the lysing protocol main menu on the Precellys Evolution tissue homogenizer by selecting appropriate tube capacity (2 mL, 7 mL or 15 mL), speed (4500–10000 rpm), number of cycles (1 to 10), cycle duration (10 to 900 s) and waiting time between two cycles (1 to 120 s). Position the lysing tubes from step 1 in appropriate tube holder (for 2 mL, 7 mL or 15 mL tubes) within the homogenizer and add the indented plate to hold the tubes in place. Close the homogenizer lid and initiate the lysing process.

Tip: In the lysing protocol, the speed, number of cycles and cycle duration need to be empirically determined for each sample or tissue type for optimal lysis and DNA recovery. Allow sufficient waiting time between two cycles to enable the unit to cool down between cycles to prevent overheating.

3. Upon completion of the lysis/homogenization protocol, transfer the lysis tubes into an appropriate biosafety cabinet.

Tip: For cell and tissue samples that were lysed in 7 mL or 15 mL homogenization tubes, transfer 1 mL of TriReagent suspension from the homogenization tube into a new 2 mL Sarstedt microfuge tube, and archive the residual suspension (aliquoted or unaliquoted) at −80 °C for potential additional analysis. Alternatively, transfer up to 2.5 mL of TriReagent suspension from the 7 mL or 15 mL homogenization tube into a new 5 mL Eppendorf microfuge tube, and archive the residual suspension (aliquoted or unaliquoted) at −80 °C for potential additional analysis. (If the latter option is taken, equipment accommodation needs to be made, such as using an Eppendorf centrifuge 5430 with rotor FA-45–16-17, to allow centrifuging 5 mL microfuge tubes at up to 21,000 xg. In addition, the volumes of all reagents in Protocol 3.1 steps 5–9, and Protocol 3.2 need to be increased proportionally). For both options, multiple aliquots can be processed for analysis if needed.

The following steps are based on 1 mL of TriReagent suspension volume.

4. Store the homogenate for 5 min at room temperature to allow complete dissociation of nucleoprotein complexes. Spin the

homogenate at 13,000 xg for 1 min, and remove top lipid layer with a pipette.
5. Add 0.1 mL 1-bromo-3-chloropropane (BCP) to the homogenate and vortex the sample vigorously for 15 s. (Alternatively, the Precellys Evolution tissue homogenizer can be used to agitate the homogenate.) Store the resulting mixture at room temperature for 15 min and then centrifuge at 14,000 xg for 15 min at 4 °C. Following centrifugation, carefully transfer the colorless upper RNA containing-aqueous phase (avoiding the interphase or organic layers) to a fresh 2 mL Sarstedt microfuge tube that contains 240 μg glycogen for RNA isolation (Protocol 3.2).
6. Add 0.5 mL DNA Back Extraction Solution to the remaining homogenate phases (i.e. interphase and phenol phase). Vortex the mixture for 15 s, and centrifuge at 4 °C for 15 min at 14,000g.
7. Prepare a fresh 2 mL Sarstedt microfuge tube containing 240 μg glycogen. After centrifugation from step 6 is finished, transfer the semi-clear aqueous phase in the homogenization tube into the glycogen-containing tube. Vortex to mix, quickly centrifuge to collect liquid, then add 0.5 mL 100% isopropanol and vortex the mixture for 5 s.
8. Centrifuge the mixture at room temperature for 10 min at 21,000 xg. Decant the supernatant. Add 0.5 mL of 70% ethanol to the DNA pellet.

(Optional) Store the tube at 4 °C overnight for salt leaching.

9. Remove ethanol and allow the DNA pellet to air dry for 5 min at room temperature. Dissolve the DNA pellet in 10 mM Tris, pH 9.0 in preparation for ddPCR testing in Protocol 3.4.

Tip: Capillary pipettes can be used to aid complete removal of ethanol and prevent loss of DNA pellet during liquid removal.

Tip: Dissolve the DNA pellet in an appropriate volume of Tris as determined by expected total DNA yield, and planned DNA input quantity at the ddPCR step.

10. Determine the DNA concentration using Nanodrop spectrophotometer.

Note: Unsheared genomic DNA can be directly used in ddPCR reactions if the loading is fewer than 0.75% of the anticipated droplets, which for mammalian DNA is up to 160 ng for a 50 μL *reaction. If the user plans to include more DNA template into each ddPCR reaction, or if potential co-localized targets (multiple targets located on the same fragment of template DNA) are present (*i.e. *downstream data analysis will be complicated by the possibility that a disproportionate fraction of droplets will each exhibit signal arising from multiple targets with unfragmented template), the DNA solution should be sonicated to fragment the DNA template (step 11). For low viral load detection and quantitation applications, DNA sonication is recommended.*

11. (Optional) Sonicate the DNA solution with a Branson SFX150 sonifier to achieve an optimal fragment length of 3 to 4 kilobase.

Tip: Alternative DNA shearing methods such as with a Covaris Adaptive Focused Acoustic instrument (Blue miniTube protocol) or a Nebulizer (ThermoFisher Scientific K7025-05) can be used.

Tip: To QC the fragmented genomic DNA, run ~ 200 ng of the sheared genomic DNA on a 0.8% agarose gel to ensure the correct size range of fragmented genomic DNA. Alternatively, run ~ 10–50 ng of sheared DNA on a high sensitivity chip on an Agilent Bioanalyzer.

3.2. Quantitative recovery of RNA from cells and animal tissues

Note: Steps 1–5 of quantitative recovery of RNA are identical to steps 1–5 of Protocol 3.1. The following steps allow completion of quantitative recovery of RNA after Protocol 3.1 step 5.

1. Add 0.5 mL of isopropanol to the RNA containing-aqueous phase and glycogen mixture obtained at Protocol 3.1 step 5. Vortex for 5 s. Store the mixture at room temperature for 5–10 min and centrifuge at 21,000 xg for 10 min at 25 °C.
2. Remove the supernatant and wash the RNA pellet by adding 0.5 mL of 70% ethanol and vortexing. Store the RNA pellet at −20 °C in ethanol overnight. Briefly centrifuge at 21,000 xg for 1 min at 25 °C. Decant the ethanol. Wash a second time with 0.5 mL 70% ethanol by vortexing.
3. Briefly centrifuge at 21,000 xg for 1 min at 25 °C. Decant the ethanol wash. Allow the RNA pellet to air dry for 5 min at room temperature. Dissolve the recovered RNA in 10 mM Tris, pH 8.0.

Tip: Capillary pipettes can be used to aid complete removal of ethanol and prevent loss of DNA pellet during liquid removal.

Tip: Dissolve the RNA pellet in an appropriate volume of Tris as determined by expected total RNA yield, and planned RNA input quantity at the reverse transcription step.

3.3. Reverse transcription with a high processivity reverse transcriptase

1. Set up the reverse transcription reaction according to the following recipe:

Component	Original	Final	μL per 15 μL reaction
MgCl2	25 mM	5 mM	3
dNTPs	25 mM	0.5 μM	0.3
DTT	100 mM	1 mM	0.15
SIVNestR01	100 μM	2 μM	0.3
PCR II w/ 0.2% Tween 20	10x	1x	1.5
RNaseOUT	40 U/μL	10 U	0.25
SSIV RT enzyme	200 U/μL	200 U	1
RNA sample or reference standard	Various	various	various
H2O			various

Note: A high processivity reverse transcriptase, SuperScript IV (SSIV) is used in the current recipe. Alternatively, M−MLV reverse transcriptase or SuperScript III (SSIII) can also be used (200 U in final reaction).

2. Run the reverse transcription reaction(s) with the following thermocycling program: 25 °C 15 min; 50 °C 10 min; 95 °C 10 min; 25 °C 30 min; 4 °C hold. (Note that this is a SSIV specific program.)

Note: If M−MLV or SSIII reverse transcriptase is used, the thermocycling program needs to be modified to: (M−MLV) 25 °C 15 min*; 37 °C 60* min*; 90 °C 30* min*; 25 °C 30* min*; 4 °C hold. Or (SSIII) 25 °C 15* min*; 50 °C 50* min*; 85 °C 5* min*; 25 °C 30* min*; 4 °C hold.*

3.4. ddPCR

Note: This part of the protocol assumes that a duplex assay (composed of a target (viral) assay and a reference assay) is being performed. The protocol can be adapted and modified through omitting and inclusion of primers and probe(s) to assess the viral target only, or to perform higher order multiplexed assay as described (Whale et al., 2016). In addition, the current protocol is based on the use of TaqMan Genotyping master mix with the incorporation of MGB probes. Additional probe systems and master mixes can be explored to empirically determine optimal performance characteristics such as assay background, cluster separation, cluster diffuseness and the agreement between signal counts vs *inputs* [19,21].

1. In 1.5 mL low binding microfuge tubes, prepare up to 8 PCR reactions (for one source run) on ice based on the following ddPCR recipe:

Component	Original	Final	µL per 50 µL reaction
TaqMan genotyping master mix	2x	1x	25
Target assay forward primer (SGag forward)	100 µM	600 nM	0.3
Target assay reverse primer (SGag reverse)	100 µM	600 nM	0.3
Target assay probe (SGag ddPCR probe)	10 µM	200 nM	1
Reference assay forward primer (RCCR5 forward)	100 µM	200 nM	0.1
Reference assay reverse primer (RCCR5 reverse)	100 µM	200 nM	0.1
Reference assay probe (RCCR5 ddPCR probe)	10 µM	200 nM	1
Droplet stabilizing solution	25x	1x	2
DNA sample or reference standard	various	various	various
H2O			various

2. Initialize the Raindance source instrument and launch the instrument control software (ICS) application.

Note: The source instrument automates the process of converting the sample prepared in step 1 to millions of picoliter droplets. Perform the source machine-related steps (2–9) in a pre-PCR environment or a dedicated laminar flow hood to avoid contamination that could lead to false positive amplification. The ddPCR assay sensitivity and lower limit of detection (LLOD) may be affected by contamination and false positive amplification.

3. Unlock the Raindance source instrument door through the "Run info" tab. Insert a new PCR tube strip into the source instrument metal holder with correct orientation.

Tip: There is a "numbered area" that indicates a unique number on each tube to help tracking the orientation of the strip tubes (i.e. *tube #1 next to "A" position as marked on the holder, and tube #8 next to "H" position).*

4. Place a new Raindance source chip on a clean, solid bench surface, and load the PCR reaction mixtures (from step 1) slowly into the bottom of the sample input wells to avoid creating air bubbles.

Caution: Avoid touching the chip's oil input gaskets, sample input wells, emulsion output nozzles, the clear microfluidic chip or imaging region at step 4.

Tip: Each well can be filled up to a maximum of 50 µL. *The loading volume for each reaction can also be reduced to* 25 µL *(this will reduce the number of droplets generated in each reaction to ~ 5 million.)*

5. Scan the chip barcode using the barcode reader which is controlled by the ICS software. Ensure the source chip information (such as lot and serial number) automatically populates the "Source chip" section of "Run Data".
6. Insert the chip into the RainDance Source instrument and properly orient the chip (guided by the alignment pins). Ensure the following indicators on the System Status screen meet "System Ready" requirement: Pressure Ready, Carrier Oil, PCR Tube Strip Inserted, Chip Inserted, Door Closed. Manually populate or import the "Run Name" and "Sample identifier" (for each lane) on the Run Data tab/screen.

Note: Gas pressure and oil status should be checked during instrument installation and routine maintenance. "Pressure Ready" indicates whether the instrument gas pressure is suitable for running an experiment. "Carrier Oil" indicates whether there is sufficient oil in the reservoir to complete the current run.

Optional: Click on the "Run Info" tab to populate operator, sample ID and run notes fields.

7. Start Run to initiate dropletization (Fig. 1).

Note: The screen displays images of the droplets as they move through the device in real time. When dropletization in all lanes is finished, the source instrument performs emulsion detection while the tube strip fills with additional oil and triggers the level sensor. After the instrument screen displays "Raindance source run completion" to indicate this step is finished, the instrument performs rinse and recovery for the next source run.

8. Remove the used chip after rinsing and recovery are complete, return it to its packaging for storage or disposal. Inspect the "Raindance source run report" displayed on screen for each channel's source run "Pass/Fail" results.
9. Cover the tube strip with the RainDrop Elastomer (standard PCR) tube strip cap with the tab to the left. Remove the tube strip from the instrument and transfer the sealed sample tube strip to a C1000 Touch Thermal Cycler (or an equivalent thermocycler).

Caution: Ensure that the cap is tightly sealed over the strip to avoid contamination and sample loss due to evaporation. Inspect the liquid in the tubes without disturbing the two phases (creamy white/opaque emulsion on the top and the clear oil on the bottom).

Tip: The source instrument run data can be retrieved from the performance log file at this step.

Note: Perform the thermocycling step in a post-PCR environment or a location that is different from where the PCR reactions were prepared (in step 1) to prevent future contamination with PCR amplicons.

10. On the C1000 Touch Thermal Cycler, run the following PCR program:

95 °C for 10 min, 40 cycles of (95 °C for 15sec followed by 60 °C 1 min), 98 °C for 10 min, 4 °C hold (with a ramp speed of 0.5 °C/second)

Critical step: The adjustable-height, texture-free, hard surface heated lid is required for the thermal cycler to ensure sufficient cover pressure to prevent evaporation and condensation. Evaporation and condensation can lead to spurious noise and clusters in ddPCR signal plot.

Note: The slow ramp speed is chosen to provide equilibrating temperature exposure across the droplet population (i.e. *heat transfers more slowly in an emulsified sample compared to a bulk PCR reaction).*

Caution: The PCR cycle is reduced to 40 cycles [20].

Note: If the thermocycler allows defining a sample volume in the program, use 75 µL, *as this is the approximate final volume of emulsion and oil that is generated on source instrument from a* 50 µL *original PCR reaction.*

11. Upon completion of the end-point PCR, remove the RainDrop Elastomer tube strip cap, and replace with a High Speed PCR Tube Strip Cap. Transfer the capped tube strip to the Sense instrument.

Note: Perform steps 12–18 in a post-PCR environment or a location different from where the PCR reactions were prepared (in step 1) to prevent future contamination with PCR amplicons.

12. Initialize the Raindance sense instrument and launch the instrument control software (ICS) application.
13. Unlock the Raindance sense instrument door through the "Run info" tab. Insert the tube strip from step 11 into the tube strip nest with the tabbed end to the left.
14. Remove a new sense chip from its packaging without touching the clear microfluidic chip, the droplet detection region, or the objective lens.

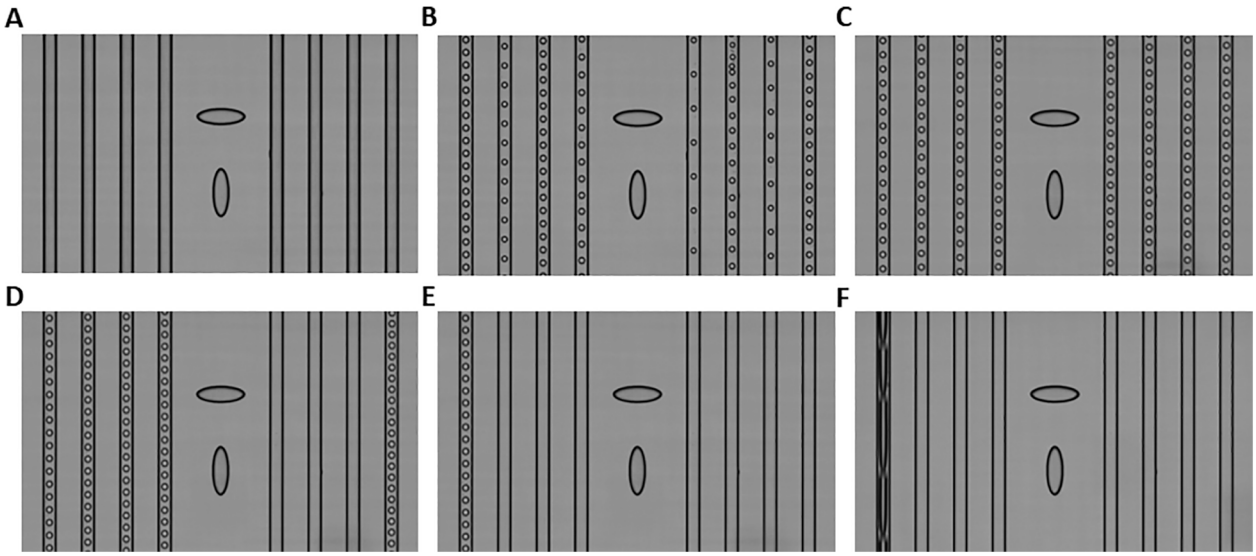

Fig. 1. Time course of oil emulsion droplet generation on a Raindance source chip. Images of droplets as displayed on the Raindance source instrument control software (ICS) interface as they are being generated and move through the device in each channel in real time. (A) Image of the channels on the source chip when the first drops from each sample are being formed and ready to enter the channels/lanes. (B) Droplet images as the Raindance source instrument is in the process of adjusting the air pressure and consequently the flow rate via a so-called "proportional-integral-derivative" feedback loop mechanism to generate 5 picoliter drops with proper size and spacing. (C) Droplets are being generated in all lanes with uniform spacing. (D) In some lanes dropletization is completed (as indicated by blank lanes). (E) In most lanes dropletization is completed. (F) Dropletization in all lanes is nearly completed. (In the first lane in (F), the elongated droplets indicate that all the sample in the lane has been dropletized, and the lane will shortly be blank.) Time elapse since the beginning of dropletization: (A) 0 min; (B) 0 min 3 s; (C) 0 min 15 s; (D) ~ 15 min; (E) ~ 16 mintues; (F) ~ 17 min.

15. Scan the sense chip barcode using the sense instrument's barcode reader. Ensure the sense chip's lot and serial number information populates in the Run Data section.
16. Insert the sense chip into the sense instrument using the instrument alignment pins as guides. Place the chip compression plate over the sense chip to ensure the chip compression plate is not movable left to right or front to back. Ensure the following indicators on the System Status screen meet "System Ready" requirement: Pressure Ready, Carrier Oil, Drive Oil, Chip Inserted, Door Closed. Manually populate or import the "Run Name" and "Sample identifier" (for each lane) on the Run Data tab/screen.

Note: Gas pressure and oil status should be checked during instrument installation or routine maintenance. "Pressure Ready" indicates whether the instrument gas pressure is suitable for running an experiment. "Carrier Oil" indicates whether there is sufficient oil in the carrier oil reservoir to complete the current run. Likewise "Drive Oil" indicates whether there is sufficient oil in the drive oil reservoir to complete the current run.

Optional: Click on the "Run Info" tab to populate operator, sample ID and run notes fields.

17. Start Run to initiate the sense run. On-screen display will indicate the sample that is being processed and its run progress. After all samples are processed, return the used chip to its packaging for storage or disposal.
18. Save or transfer the run files (in .fcs data format) for data analysis.

Note: "Run Report" contains key statistics such as the droplet count for each sample (Fig. 2).

3.5. Data analysis and report generation

1. Launch the RainDrop Analyst II software. Drag and drop the raw sense data files (i.e. fcs files retrieved from the Raindance sense instrument at the end of Procedure 3.4), up to 8 files in a batch analysis, into the Workspace "Sample View" space. Select the fcs data file(s) that requires spectral compensation in Sample View.

*Note: The spectral compensation function of the software is to correct for the overlapping signals (*i.e. *spillover) between the two photomultiplier tubes (PMTs) on the RainDrop Sense instrument. Data files generated under the same reaction condition and during the same Sense instrument run can be compensated with the same matrix.*

2. Select one of the fcs data files in "Sample View" to allow "Intact droplets" number and statistics info to populate the "Analysis View" space in the Workspace, and a PMT1 vs. PMT2 scatter plot (graph plot) to populate the main (center and upper right) space of the Workspace. In the Axis Options space (center and lower right), manually update the axis scale minimum and maximum values so that the corresponding graph includes all droplet data.

Tip: In case a group of fcs data files are being analyzed, the axis scale minimum and maximum values should be set to be identical across all fcs files such that all droplet data on all data files are covered (except outlier data points that a user chooses not to include in the analysis).

3. To initiate spectral compensation, in the graph plot, add a gate to each cluster by first selecting a gate shape at the top of the "Graph Details" panel (e.g., a rectangle), and then draw the shape (i.e. gate) around the cluster to ensure most or all the droplets within the cluster fall within the shape. Name each gate as appropriate, such as the follows: "Negative", "Dye 1 X axis" and "Dye 2 Y axis". Once gating is complete, click on "Apply Spectral Compensation". In the "Spectral Compensation" dialog box that appear, choose "Use Calculated matrix", and select appropriate gate names from the dropdown menu, i.e. "Negative" for "Negative Population", "Dye 1 X axis" for "Dye 1(X-Axis)", "Dye 2 Y axis" for "Dye 2(Y-Axis)".

Tip: The same compensation matrix can be applied to multiple fcs data files by selecting the "Apply Spectral Compensation to Selected Samples" check box.

A

Chip lane	Intact droplet detected	QC droplets	QC/intact detected (%)	Template/sample	Condition test	Animal ID
1a	9,077,768	111,081	1.22	Lymph node CD4 CM T cell DNA (800 cells) (SIV infected) with SIV DNA preamplified	Preamplified template test, non-suppressed viral load test [19,20]	311-04
1b	9,057,512	109,432	1.21	Lymph node CD4 CM T cell DNA (80 cells) (SIV infected) with SIV DNA preamplified	Preamplified template test, non-suppressed viral load test [19,20]	311-04
1c	9,103,021	106,514	1.17	500 copies of SIV DNA standard in buffer	Standard spike test, input test [19]	n/a
1d	8,515,751	106,300	1.25	5000 copies of SIV DNA standard in buffer	Standard spike test, input test [19]	n/a
1e	8,966,851	102,703	1.15	50000 copies of SIV DNA standard in buffer	Standard spike test, input test [19]	n/a
1f	8,484,946	102,904	1.21	Ovary DNA (2 million cell equivalent) (SIV infected, ART suppressed)	Non-preamplified, tissue-derived template test, input test [19]	313-08
1g	8,917,794	107,573	1.21	Ovary DNA (0.5 million cell equivalent) (SIV infected, ART suppressed)	Non-preamplified, tissue-derived template test, input test [19]	313-08
1h	8,178,223	107,561	1.32	Ovary DNA (0.125 million cell equivalent) (SIV infected, ART suppressed)	Non-preamplified, tissue-derived template test, input test [19]	313-08
2a	9,171,275	117,852	1.29	Uterus DNA (1 million cell equivalent) (SIV infected, ART suppressed)	Assay primer & probe concentration test [20]	313-08
2b	8,545,175	118,565	1.39	Uterus DNA (1 million cell equivalent) (SIV infected, ART suppressed)	Assay primer & probe concentration test [20]	313-08
2c	9,070,925	116,370	1.28	Uterus DNA (1 million cell equivalent) (SIV infected, ART suppressed)	Assay primer & probe concentration test [20]	313-08
2d	9,011,300	115,301	1.28	Uterus DNA (1 million cell equivalent) (SIV infected, ART suppressed)	Assay primer & probe concentration test [20]	313-08
2e	8,393,050	111,431	1.33	Uterus DNA (1 million cell equivalent) (SIV infected, ART suppressed)	Assay primer & probe concentration test [20]	313-08
2f	8,580,425	111,933	1.30	Uterus DNA (1 million cell equivalent) (SIV infected, ART suppressed)	Assay primer & probe concentration test [20]	313-08
2g	8,731,550	115,494	1.32	Uterus DNA (1 million cell equivalent) (SIV infected, ART suppressed)	Assay primer & probe concentration test [20]	313-08
2h	8,461,850	118,837	1.40	Uterus DNA (1 million cell equivalent) (SIV infected, ART suppressed)	Assay primer & probe concentration test [20]	313-08
3a	9,232,701	119,154	1.29	Ovary DNA (1 million cell equivalent) (SIV infected, ART suppressed)	Tissue-derived DNA (from ART-suppresed Rhesus macaque) input test	311-08
3b	8,714,985	118,873	1.36	Ovary DNA (1 million cell equivalent) (SIV infected, ART suppressed)	Tissue-derived DNA (from ART-suppresed Rhesus macaque) input test	311-08
3c	9,314,949	115,660	1.24	Ovary DNA (2 million cell equivalent) (SIV infected, ART suppressed)	Tissue-derived DNA (from ART-suppresed Rhesus macaque) input test	311-08
3d	8,230,842	113,120	1.37	Ovary DNA (2 million cell equivalent) (SIV infected, ART suppressed)	Tissue-derived DNA (from ART-suppresed Rhesus macaque) input test	311-08
3e	8,467,677	110,414	1.30	Ovary DNA (2.5 million cell equivalent) (SIV infected, ART suppressed)	Tissue-derived DNA (from ART-suppresed Rhesus macaque) input test	311-08
3f	8,508,142	110,900	1.30	Ovary DNA (2.5 million cell equivalent) (SIV infected, ART suppressed)	Tissue-derived DNA (from ART-suppresed Rhesus macaque) input test	311-08
3g	8,714,843	116,400	1.34	Ovary DNA (3 million cell equivalent) (SIV infected, ART suppressed)	Tissue-derived DNA (from ART-suppresed Rhesus macaque) input test	311-08
3h	8,144,459	117,420	1.44	Ovary DNA (3 million cell equivalent) (SIV infected, ART suppressed)	Tissue-derived DNA (from ART-suppresed Rhesus macaque) input test	311-08
4a	8,605,993	108,120	1.26	Buffer spike (0 copy of SIV RNA standard) in 1 µg naïve animal PBMC RNA	RT enzyme, amount and priming method test (M-MLV, gene specific priming) [26]	n/a
4b	8,152,299	108,375	1.33	100 copies of SIV RNA standard spiked in 1 µg naïve animal PBMC RNA	RT enzyme, amount and priming method test (M-MLV, gene specific priming) [26]	n/a
4c	8,480,053	102,165	1.20	Buffer spike (0 copy of SIV RNA standard) in 1 µg naïve animal PBMC RNA	RT enzyme, amount and priming method test (SSIII(low), random hexamer priming) [26]	n/a
4d	8,550,991	102,770	1.20	100 copies of SIV RNA standard spiked in 1 µg naïve animal PBMC RNA	RT enzyme, amount and priming method test (SSIII(low), random hexamer priming) [26]	n/a
4e	7,641,077	96,582	1.26	Buffer spike (0 copy of SIV RNA standard) in 1 µg naïve animal PBMC RNA	RT enzyme, amount and priming method test (SSIII(high), random hexamer priming)[26]	n/a
4f	7,817,625	94,981	1.21	100 copies of SIV RNA standard spiked in 1 µg naïve animal PBMC RNA	RT enzyme, amount and priming method test (SSIII(high), random hexamer priming) [26]	n/a
4g	7,343,166	101,215	1.38	Buffer spike (0 copy of SIV RNA standard) in 1 µg naïve animal PBMC RNA	RT enzyme, amount and priming method test (SSIII(low), gene specific priming) [26]	n/a
4h	8,251,560	102,042	1.24	100 copies of SIV RNA standard spiked in 1 µg naïve animal PBMC RNA	RT enzyme, amount and priming method test (SSIII(low), gene specific priming)[26]	n/a
5a	8,507,329	117,881	1.39	Buffer spike (0 copy of SIV RNA standard) in buffer	Assay background test, PCR step primer and probe concentration test (M-MLV) [19,26]	n/a
5b	8,312,509	121,247	1.46	Buffer spike (0 copy of SIV RNA standard) in buffer	Assay background test, PCR step primer and probe concentration test (M-MLV) [19,26]	n/a
5c	8,210,718	119,758	1.46	Buffer spike (0 copy of SIV RNA standard) in buffer	RT enzyme test, RNA background test (M-MLV) [19,26]	n/a
5d	7,868,307	117,713	1.50	10 copies of SIV RNA standard spiked in buffer	RT enzyme test, RNA background test (M-MLV) [19,26]	n/a
5e	8,457,749	112,854	1.33	Buffer spike (0 copy of SIV RNA standard) in 1 µg naïve animal PBMC RNA	RT enzyme test, RNA background test (M-MLV) [19,26]	n/a
5f	8,216,848	114,230	1.39	10 copies of SIV RNA standard spiked in 1 µg naïve animal PBMC RNA	RT enzyme test, RNA background test (M-MLV) [19,26]	n/a
5g	7,889,980	117,097	1.48	Buffer spike (0 copy of SIV RNA standard) in 1 µg naïve animal PBMC RNA	RT enzyme test, RNA background test (SSIII (low)) [19,26]	n/a
5h	7,606,745	118,334	1.56	10 copies of SIV RNA standard spiked in 1 µg naïve animal PBMC RNA	RT enzyme test, RNA background test (SSIII (low)) [19,26]	n/a
6a	8,308,729	121,273	1.46	Buffer spike (0 copy of SIV RNA standard) in 1 µg naïve animal PBMC RNA	high processivity RT enzyme (SSIV) test [19,26]	n/a
6b	7,863,279	123,607	1.57	10 copies of SIV RNA standard spiked in 1 µg naïve animal PBMC RNA	high processivity RT enzyme (SSIV) test [19,26]	n/a
6c	7,598,391	120,564	1.59	Buffer spike (0 copy of SIV RNA standard) in 1 µg naïve animal PBMC RNA	high processivity RT enzyme (SSIV) test [19,26]	n/a
6d	7,695,364	117,649	1.53	10 copies of SIV RNA standard spiked in 1 µg naïve animal PBMC RNA	high processivity RT enzyme (SSIV) test [19,26]	n/a
6e	8,072,779	115,563	1.43	1000 copies of SIV RNA standard spiked in 100 ng bone marrow RNA	high processivity RT enzyme (SSIV) test, challenging sample type test [19,26]	29676
6f	7,738,131	115,381	1.49	1000 copies of SIV RNA standard spiked in 10 ng bone marrow RNA	high processivity RT enzyme (SSIV) test, challenging sample type test [19,26]	29676
6g	7,402,558	122,731	1.66	10 copies of SIV RNA standard spiked in 1 µg naïve animal PBMC RNA	Enzyme processivity comparison test (M-MLV) [19,26]	n/a
6h	7,892,599	116,560	1.48	10 copies of SIV RNA standard spiked in 1 µg naïve animal PBMC RNA	Enzyme processivity comparison test (SSIII) [19,26]	n/a

B

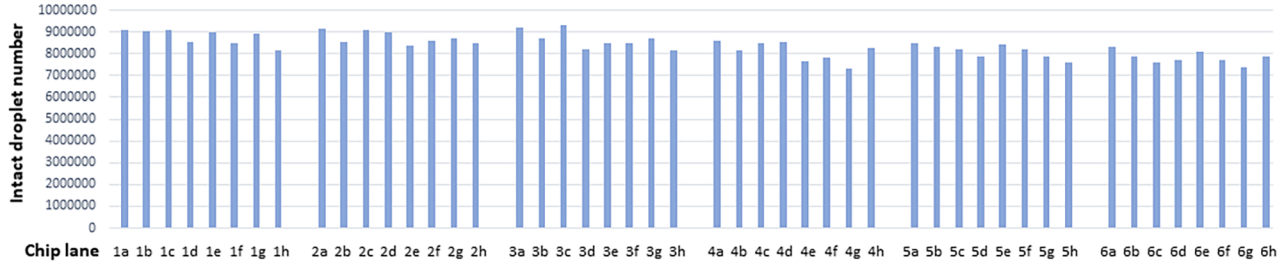

C

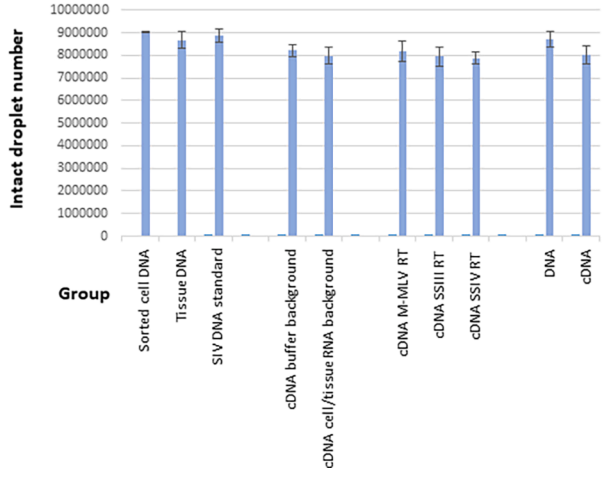

D

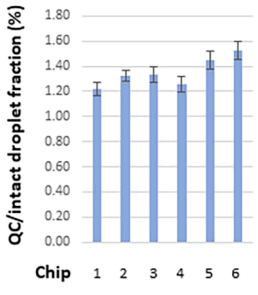

(caption on next page)

Fig. 2. Summary of the numbers of droplets that were successfully imaged on the sense chips under various test conditions and with a variety of sample types. (A) A detailed description of the numbers of intact droplets detected during fluorescence imaging on the sense instrument, the corresponding numbers of quality control (QC) droplets (representing a fraction of the total droplets generated for each lane) during dropletization on the source instrument, the QC/intact droplet fraction, samples and test conditions, and animal IDs (if applicable). Chip 1–3 results were based on DNA templates, and chip 4–6 results were based on cDNA templates. *(Chip 1)* Samples tested included preamplified cell DNA from an animal infected with SIV (no ART suppression) (a and b), SIV DNA standard spike (c-e), and non-preamplified tissue DNA from an SIV-infected animal subject to ART suppression (f-g) [19,21]. CM T cell: central memory T cell. ART: antiretroviral therapy. *(Chip 2)* Assay primer and probe concentration tests on tissue-derived DNA template from an SIV-infected animal subject to ART suppression [21]. Primer and probe concentration (in nM) variations tested (in the order of SGag forward, SGag reverse, SGag ddPCR probe, RCCR5 forward, RCCR5 reverse, RCCR5 ddPCR probe) were: (a) 600, 600, 200, 400, 400, 200; (b) 600, 600, 200, 600, 600, 200; (c) 600, 600, 200, 200, 200, 200 (the standard condition as indicated in section 3.4 ddPCR recipe); (d) 600, 600, 200, 200, 200, 100; (e) 600, 600, 100, 400, 400, 200; (f) 600, 600, 100, 600, 600, 200; (g) 600, 600, 100, 200, 200, 200; (h) 600, 600, 100, 200, 200, 100. *(Chip 3)* Tissue-derived DNA input tests. 1 million to 3 million cell equivalent DNA derived from the ovary tissue from an SIV-infected, ART suppressed Rhesus macaque were subject to ddPCR analysis. *(Chip 4)* Reverse transcriptase enzyme, amount and priming strategy tests. PBMC: peripheral blood mononuclear cell. M−MLV, 200 units (per manufacturer definition) of the M−MLV reverse transcriptase in each reverse transcription reaction. SSIII(low), 20 units (per manufacturer definition) of the SuperScript III reverse transcriptase in each reverse transcription reaction. SSIII(high), 200 units of the SuperScript III reverse transcriptase in each reverse transcription reaction. *(Chip 5)* Assay background and reverse transcriptase tests. Assay background (no template control) tests were performed both in buffer background (a-c) and in the background of RNA extracted from PBMCs from a naïve animal (e and g). M−MLV, 200 units (per manufacturer definition) of the M−MLV reverse transcriptase in each reverse transcription reaction. SSIII(low), 20 units (per manufacturer definition) of the SuperScript III reverse transcriptase in each reverse transcription reaction. *(Chip 6)* Enzyme processivity tests and bone marrow test. Performances of 3 reverse transcriptases with different processivity at low RNA template input were compared (a-d, g and h). In addition, the performance of the SSIV reverse transcriptase in the background of RNA derived from a high fat content tissue (i.e. bone marrow) was evaluated. The number of intact droplets detected at the sense step on chips 1–6 on average was 99.6 ± 1.2% of the number of total droplets detected at the sense instrument step. (B) Intact droplet number for each individual lane as plotted based on (A). (C) Group comparison of intact droplet numbers based on (A) and (B). The numeric values are: Sorted cell DNA group (1a, 1b), n = 2, average = 9,067,640, range = 9,057,512–9,077,768; tissue DNA group (1f-1h, 2a-2h, 3a-3h), n = 19, 8,677,637 ± 356,302; SIV DNA standard group (1c-1e), n = 3, 8,861,874 ± 307,387. cDNA buffer background group (5a-5d), n = 4, 8,224,716 ± 267,582; cDNA cell/tissue RNA background group (4a-4h, 5e-5h, 6a-6h), n = 20, 7,979,296 ± 384,328. cDNA M−MLV reverse transcriptase (RT) group (4a, 4b, 5e, 5f, 6g), n = 5, 8,167,089 ± 464,845; cDNA SSIII RT group (4c-4h, 5g, 5h, 6h), n = 9, 7,941,533 ± 409,018; cDNA SSIV RT group (6a-6f), n = 6, 7,879,446 ± 266,372. DNA group (1a-1h, 2a-2h, 3a-3h), n = 24, 8,733,167 ± 349,305; cDNA group (4a-4h, 5a-5h, 6a-6h), n = 24, 8,020,199 ± 374,283. Although not statistically significant, there was a trend which suggested that lanes that contained DNA templates as the input on average had greater intact droplet numbers than lanes that contained cDNA templates as the input. (D) Comparison of the QC droplets/intact droplets factions (in %) among the 6 chips based on (A). The numeric values are: chip 1, n = 8, 1.22 ± 0.05; chip 2, n = 8, 1.32 ± 0.05; chip 3, n = 8, 1.33 ± 0.06; chip 4, n = 8, 1.26 ± 0.06; chip 5, n = 8, 1.45 ± 0.07; chip 6, 1.53 ± 0.08.

*Tip: Spectral compensation can alternatively be performed through loading a previously saved matrix in a user-defined Spectral Compensation Library by choosing "Compensated Matrix Options" to load the matrix. At this step, the dialog box also allows customizing axis names (*e.g. *such as with probe dye names).*

Tip: For assays with clean background, the corresponding gated areas in control sample(s) are expected to be completely void of target signal(s).

4. To add a statistic to a population, select the population in the Analysis View, and then choose the statistics function in the Toolbar Ribbon. Using the "Add Statistic" dialog window, select and add the Statistics and the Parameters.

Tip: Multiple items in each category can be selected and added.

Tip: Statistics can be copied from one fcs data file to other fcs data files in the Workspace by first selecting the target fcs data files in the Sample View. Highlight the analyzed sample in the Sample View, then select the top-level population in the Analysis View and choose 'Apply Gates and Statistics to Selected Samples'.

Tip: Statistics can be copied from one population to another by using the 'Copy All Statistics" function.

Critical step: Poisson correction and ratio statistics require specification of respective populations

5. Upon completion of data analysis, select the 'Reports' tab on the top of the Workspace. Choose 'New Report Template'. Tabs above the blank report editor allow modifying different sections of the report. The Report Toolbar Ribbon allows adding objects to each report section. Use 'Generate Report' function to generate a pdf report for the selected fcs data files. Select the "Graph Details" view and the "Export Graph" function to export a graph. To export multiple graphs, select the "Multiple Samples" View, and use the 'Export' function. To export all data in a .csv file format, select 'Export Analysis' from the Workspace menu item. Then save the Workspace for potential future analysis.

*Tip: Potential objects allowed in the report include text, images, summary data graphs, individual data graphs, data tables, and statistics. Different report sections allow different objects. The "Header and Footer" sections allow text and images. The "Summary Content" section allows summary graphs and summary statistics (*i.e. *data tables). "Per-Sample Content" allows text, images, individual graphs and statistics, and the "Conclusion" section only allows text and Images. Information on any object can be edited by using the 'Edit Report Item Property' function.*

Tip: The '3D View' function within the Toolbar Ribbon allows generating a 3D image for the population selected within the Analysis View. The X-axis and Y-axis scales are the same as in 2D plots, and the Z-axis represents droplet count on a log *scale.*

4. Results

4.1. Droplet generation

In Fig. 1, images of droplets (based on genomic DNA template inputs) were captured as they were being generated and moved through the Raindance source device channels in real time (Fig. 1). A similar droplet generation time course was observed when cDNA was used as the template at the dropletization step in a two-step RT-ddPCR procedure (however, see 4.2). The uniform spherical shape of the droplets and their regular spacing indicate proper droplet formation/breakup during dropletization. Dropletization is completed in some lanes slightly earlier than in other lanes. One possible contributing factor is the small variation in the starting reaction volumes that were loaded into each of the lanes on the same chip.

Droplet physical integrity after the source step is important as properly formed droplets provide the microenvironment for downstream PCR reaction and imaging steps. We observed that the emulsion droplet integrity and droplet numbers remain relatively stable up to 8 million cell equivalent DNA input per 50 μL reaction (Fig. 2A, chip 3; [20]), based on QC droplet counts on the source instrument (see 4.2). (Droplet integrity for an DNA input of higher than 8 million cell equivalent DNA per reaction was not tested, as we detected reaction inhibition when more than 4 million cell equivalent DNA was used in

each reaction [20].) In comparison, on the Bio-Rad ddPCR platform, droplet deformation and number decrease became obvious when DNA input was increased to 3 μg (corresponding to 0.45 million cell equivalent) in each reaction [58].

4.2. Number of intact droplets that were imaged at the "sense" step under different test conditions and with various sample input types

The number of intact droplets imaged at the fluorescent detection step during the "sense" run is a parameter that can contribute significantly to the sensitivity of sample analysis. This parameter is potentially important in suppressive ART-treatment scenarios where it is critical to differentiate between authentic, low level viral signal (e.g. single digit level viral signal in 10 million cells) and no target signals, as a significant loss in intact droplet number (i.e. compared to the theoretical number based on input volume) can create uncertainty in result interpretation, especially when no viral signal is detected. We examined the effect of various sample types and experimental conditions on the number of intact droplets. These include DNA samples extracted from a small number of sorted cells (Fig. 2A, lanes 1a &b) and different quantities of tissues (ranging from 0.125 million cell equivalent to 3 million cell equivalent) (Fig. 2A, lanes 1f-h, 2a-h, 3a-h), and SIV DNA standard (Fig. 2A, lanes 1c-e); and cDNAs derived from SIV RNA standard in buffer, or in cell/tissue-derived Rhesus macaque RNA background (Fig. 2A, lanes 4a-h, 5a-h, 6a-h).

When DNA was used as the input, we did not observe detectable differences in droplet numbers among the three sample type groups, namely sorted cells, tissues, and SIV DNA standard (Fig. 2C). We also did not observe any effect of tissue DNA input quantity on droplet number (Fig. 2A, lanes 3a-h) in the DNA quantity range tested. Similarly, when cDNA samples were used as the input, we did not detect a significant difference in droplet numbers between the group in buffer background and the group in cell/tissue RNA background (Fig. 2C). We further divided the tissue/cell RNA background group by the reverse transcriptases used during the reverse transcription step leading to cDNA generation. Different reverse transcriptases led to similar droplet numbers (Fig. 2C). We did observe that, although not statistically significant, there was a trend which suggested that reactions that used DNA templates yielded greater intact droplet numbers at the imaging step compared to reactions that contained cDNA templates (Fig. 2C).

Although the Raindance ddPCR platform "source" (i.e. dropletization) instrument is supposed to generate 10 million droplets for each 50 μL starting reaction volume, this is rarely obtainable due to dead/lost volume, the portion of the internal volume out of the microfluidic flow path. Another factor that can potentially contribute to the number of intact droplets is the components in the input sample which could potentially influence the emulsion step. For example, it is known that sample viscosity plays a critical role in emulsification through potentially interfering with average droplet volume and droplet number as well as the dynamics of droplet stability [59]. As the cDNA templates used in the current testing protocol were not purified after the reverse transcription step, the reagents (e.g. glycerol) carried over from the reverse transcription step could potentially contribute to the slightly lower droplet numbers observed compared to when DNA templates were used, assuming the difference among the numbers of imaged droplets mirrors the difference in the numbers of droplets generated at the dropletization step. It is noteworthy that this assumption requires confirmation, as the "source" machine currently does not provide the total number of droplets generated, and only provides a quality control (QC) droplet count value for each lane after dropletization (Fig. 2A). The QC droplet count value for each lane represents an estimated 1.1–1.7% of the total droplets that arrive at the imaging step, and this fraction appears to be relatively stable among the lanes within the same chip, but can vary significantly among plates (Fig. 2D), precluding a systematic analysis of the correlation between the droplet numbers after the dropletization step and after the imaging step. It also remains possible that

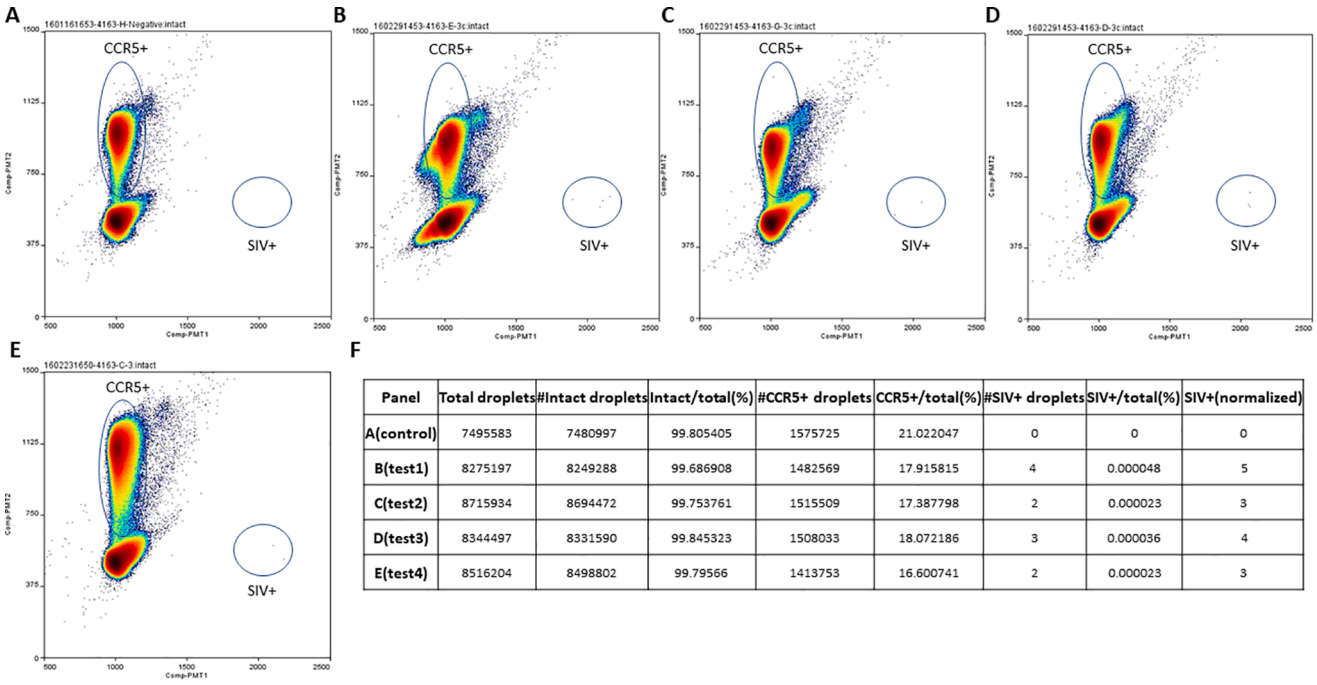

Panel	Total droplets	#Intact droplets	Intact/total(%)	#CCR5+ droplets	CCR5+/total(%)	#SIV+ droplets	SIV+/total(%)	SIV+(normalized)
A(control)	7495583	7480997	99.805405	1575725	21.022047	0	0	0
B(test1)	8275197	8249288	99.686908	1482569	17.915815	4	0.000048	5
C(test2)	8715934	8694472	99.753761	1515509	17.387798	2	0.000023	3
D(test3)	8344497	8331590	99.845323	1508033	18.072186	3	0.000036	4
E(test4)	8516204	8498802	99.79566	1413753	16.600741	2	0.000023	3

Fig. 3. Low level SIV DNA signal detection on the Raindance platform using the SIV ddPCR assay. (A) A negative control sample which contains genomic DNA extracted from 1 million Rhesus macaque peripheral blood mononuclear cells (PBMC) from a naïve (i.e. uninfected) animal. (B-E) each corresponds to an average of 3 copies of SIV DNA standard spiked in genomic DNA extracted from 1 million Rhesus macaque PBMC from the same naïve animal as in (A). "CCR5+" and "SIV+" indicate CCR5 positive and SIV positive droplets, respectively. (F) Quantitation and statistics data corresponding to (A-E). The normalized SIV + values were calculated based on duplex Poisson adjustment as described in [20]. The average SIV + value for (B-E) was 4, and the coefficient of variation (CV) was 25.5%. Note that at the 3-copy target input level, the exact copies of the target templates that are present in the reactions follow a Poisson distribution, due to the stochastic limitations inherent in target sequence distribution in the volume of sample aliquots taken for testing.

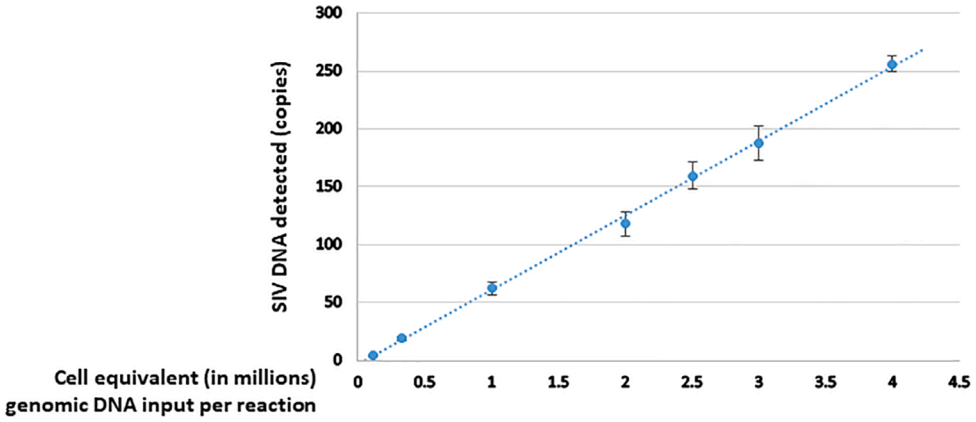

Fig. 4. Dynamic range of the SIV DNA ddPCR assay on DNA derived from a tissue sample. DNA (in quantities from 0.11 million cell equivalent to 4 million cell equivalent genomic DNA) extracted from the ovary tissue of an SIV-infected, cART suppressed Rhesus macaque, was analyzed for SIV DNA with the SIV ddPCR assay on the Raindance platform. The DNA input upper limit tested in each reaction was 4 million cell equivalent genomic DNA, as DNA input higher than this amount was shown to cause reaction inhibition [20]. The numeric values for measured DNA viral loads were: 0.11 million cell equivalent input, n = 3, 4 ± 1; 0.33 million cell equivalent input, n = 3, 19 ± 2; 1 million cell equivalent input, n = 3, 62 ± 5; 2 million cell equivalent input, n = 2, 118 (range 110–125); 2.5 million cell equivalent input, n = 2, 160 (range 151–168); 3 million cell equivalent input, n = 2, 188 (range 177–198); 4 million cell equivalent input, n = 2, 256 (range 251–261). Note that for 2 to 4 million cell equivalent DNA input, each input was tested in duplicate due to total sample quantity limitation.

the reagents carried over from the reverse transcription reaction could further affect droplet stability and number during downstream PCR and imaging steps, leading to an overall droplet number reduction.

4.3. Low level SIV DNA signal detection using the Raindance SIV ddPCR assay

The performance characteristics of the SIV ddPCR assay has been described in [20]. In Fig. 3, we show an example of low level SIV DNA signal quantification using this assay on the Raindance platform. In 3B-E, an average of 3 copies of SIV DNA standard were aliquoted into each reaction that contains background genomic DNA from 1 million Rhesus macaque peripheral blood mononuclear cells (PBMC) from an uninfected animal. After dropletization, end-point PCR and imaging, we analyzed the data as described in 3.5, and summarized the statistics and quantitation data in Fig. 3F. The average SIV copies measured were 4, with a coefficient of variation (CV) of 25.5%. It is noteworthy that at the 3-copy target input level in each reaction, the exact quantity of the target templates that are transferred into each reaction during reaction setup follows a Poisson distribution, due to the stochastic limitations inherent in target distribution in the volume of sample aliquots taken for testing.

4.4. SIV ddPCR assay dynamic range in tissue-derived DNA

We previously determined the linear dynamic range of the SIV DNA ddPCR assay to be at least 1 million copies (test upper limit) of viral nucleic acid per reaction by spiking a serial dilution of viral DNA templates of known quantities into background genomic DNA extracted from uninfected naïve Rhesus macaque PBMCs [20]. To test the performance of the assay in tissue-derived DNA samples, we analyzed the SIV viral load in a DNA sample extracted from the ovary tissue from an SIV-infected, cART-suppressed Rhesus macaque. Within the tissue DNA quantity range tested (0.11 million to 4 million cell equivalent genomic DNA per reaction, corresponding to 0.73 μg to 26.4 μg input DNA per reaction), no inhibition was observed and the assay remained linear (Fig. 4). Reaction inhibition was observed when tissue DNA input was above 4 million cell equivalent DNA in each 50 μL reaction [20].

4.5. SIV ddPCR viral quantitation in Rhesus macaque tissues at high nucleic acid input levels

The ability to tolerate a large quantity of DNA template suggests that the Raindance ddPCR platform can be routinely used to analyze tissue samples from cART-suppressed animals, as reliable detection and quantification of low-level viruses in such samples require a level of nucleic acid input that often proves to be inhibitory in qPCR reactions. Using the ddPCR assay, we tested the SIV DNA viral load in several tissue samples (including bladder, colon and liver) from an SIV-infected, ART suppressed animal at an input level of up to 3.3 million cell equivalent DNA per reaction (i.e. below the 4 million cell equivalent DNA input threshold level) when the tissue DNA amount allowed (Fig. 5). Under such conditions, triplicate reactions correspond to analyzing up to ~ 10 million cell equivalent DNA from each tissue sample. We also compared the ddPCR quantification results to those obtained with multi-reaction qPCR [55,56] when sample quantities allowed such comparisons (Fig. 5G). In the liver sample case, we included DNA samples extracted from different tissue sections of the same SIV-infected, ART-suppressed animal, and these samples showed different SIV DNA viral loads (Fig. 5B-D). In general, we observed that the ddPCR quantification results were higher (average 3.0 fold, range 1.7–5.7 fold) than the qPCR results, suggesting there was still inhibition in the qPCR reactions, although in the qPCR testing procedure the DNA samples usually have already been diluted. We previously also used the SIV ddPCR assay to quantify viral load in brain tissues from an SIV-infected, cART-suppressed Rhesus macaque, demonstrating the utility of the protocol in analyzing DNA from a tissue with high-fat content [20].

4.6. Low level SIV RNA signal detection using the Raindance SIV RT-ddPCR assay

The performance characteristics of the SIV RT-ddPCR assay, including assay dynamic range, has been described in [19,27]. The linear dynamic range of the assay was determined to be at least up to 1 million copies (test upper limit) of viral nucleic acid per reaction [20]. In Fig. 6, we show an example of low level SIV RNA signal quantification using this assay on the Raindance platform. In 6B-E, an average of 5 copies of SIV RNA standard were aliquoted into each reaction that contained 1 μg background RNA extracted from the peripheral blood mononuclear cells (PBMC) from a naïve (i.e. uninfected) animal. After reverse transcription, dropletization, end-point PCR and imaging, we analyzed the data as described in 3.5, and summarized the statistics and quantitation data in Fig. 6F. The average SIV RNA copies measured were 6, with a coefficient of variation (CV) of 26.1%. Similar to the 3-copy DNA target input case as described above, at the 5-copy RNA target input level in each reaction, the exact quantity of the target templates that are transferred into each reaction during reaction setup also follows a Poisson distribution, due to the stochastic limitations inherent in target

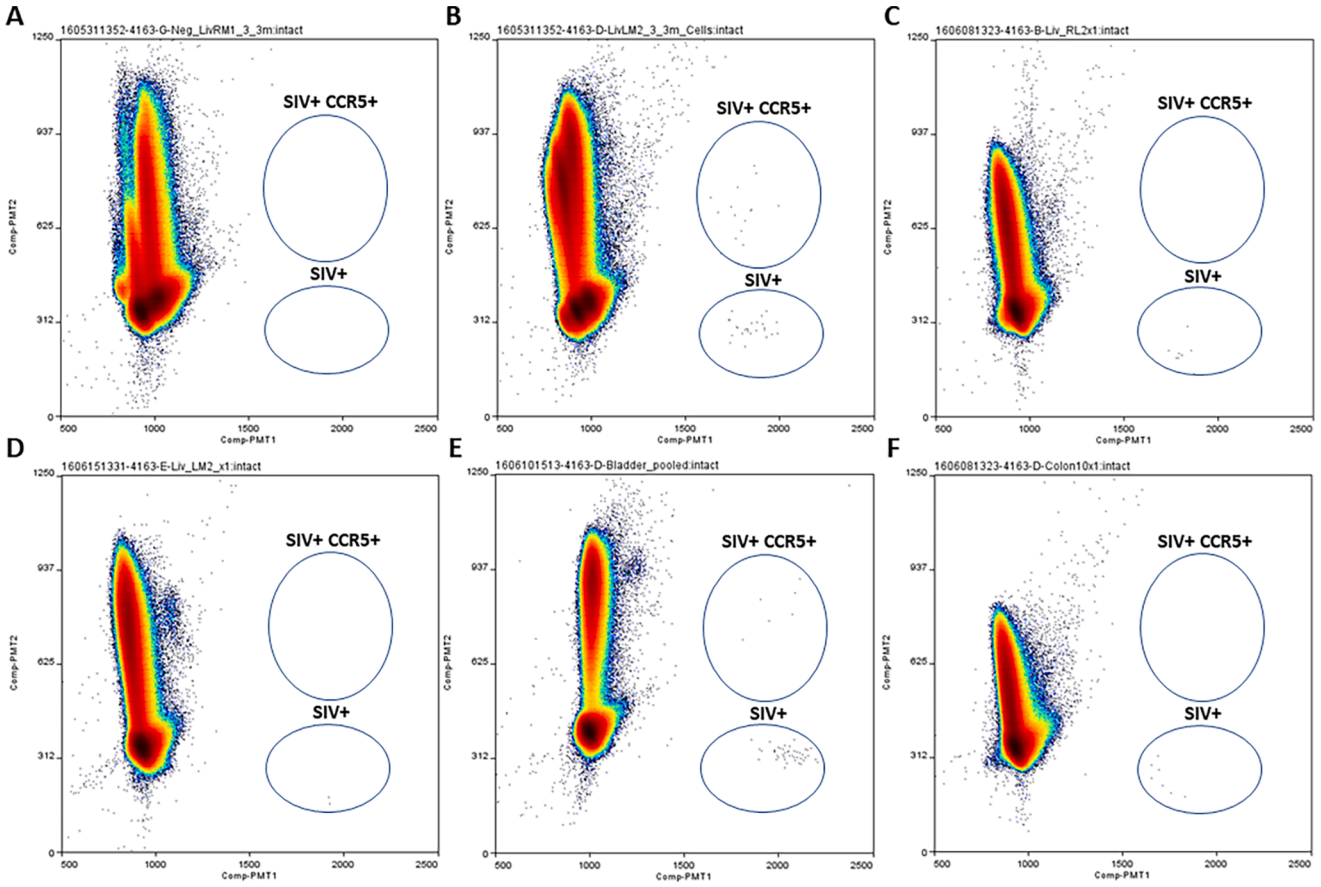

G

Panel	Tissue	Cell equivalent DNA input per reaction	Reaction replicate(s)	ddPCR viral load (copies/million cells)	qPCR viral load (copies/million cells)
A	Liver (negative control)	3.3 million	1	0	0
B	Liver	3.3 million	3	17±2	3
C	Liver	3.3 million	3	5±0	2
D	Liver	3.3 million	1	1.2	0.6
E	Bladder	1.2 million	3	55±1	32
F	Colon	3.3 million	3	3±1	1

Fig. 5. SIV ddPCR viral quantitation in Rhesus macaque tissues at high nucleic acid input levels. ddPCR viral load measurement in DNA samples derived from up to 3.3 million cell equivalent of tissue samples (all from an SIV-infected and ART suppressed animal (#27882)) in each reaction. Reactions were performed in triplicates when sample quantity allowed. "SIV+" and "SIV + CCR5+" indicate SIV positive and SIV & CCR5 double positive droplets, respectively. qPCR viral load data in the same samples were obtained using an approach where the DNA samples were diluted, and tested in up to 10 replicate reactions per sample, and quantitative viral load results derived either from SIV DNA standard curve (when all 10 reactions were PCR positive) or based on Possion statistics (when some of the reactions were PCR negative), as described in [48,56]. Note that the liver DNA samples (B-D) were from 3 different tissue sections (LM2, RL2x1 and LM2x1, respectively). Samples details and quantitation results are summarized in (G).

distribution in the volume of sample aliquots taken for testing. We previously also used the SIV RT-ddPCR assay to overcome severe viral quantitation inhibition in RNA derived from heparin-treated, Rhesus macaque bone marrow samples [20]. The inhibition in those bone marrow samples was likely due to a combination of the fat content in the bone marrow tissue, and the inhibitory effect of heparin on both the reverse transcription and PCR steps. This result demonstrated the utility of the SIV RT-ddPCR assay for analyzing RNA samples in which inhibitors were present.

5. Discussion

In this report, we developed a step-by-step protocol based on several of our previous studies describing quantitative recovery of nucleic acids from Rhesus macaque cells and tissues [55,56], Raindance ddPCR quantification of viral DNA [20,21] and Raindance RT-ddPCR quantification of viral RNA [20,27], respectively. In [55] and [56], quantitative recovery of nucleic acids was combined with a qPCR protocol which first applied a nested PCR-based preamplification reaction to enrich the specific viral target. The protocol often required sample dilution before the preamplification step and repeat testing to identify and assay under input conditions that were not inhibitory. Consequently, the qPCR protocol could accommodate a relatively small quantity of nucleic acid template in each reaction. In contrast, with properly designed, validated and optimized ddPCR and RT-ddPCR assays, the Raindance platform can enable detection of single-digit copy level viral DNA and RNA target molecules respectively, without the need for a preamplification step. This greatly simplifies workflow, minimizes hands-on steps and reduces

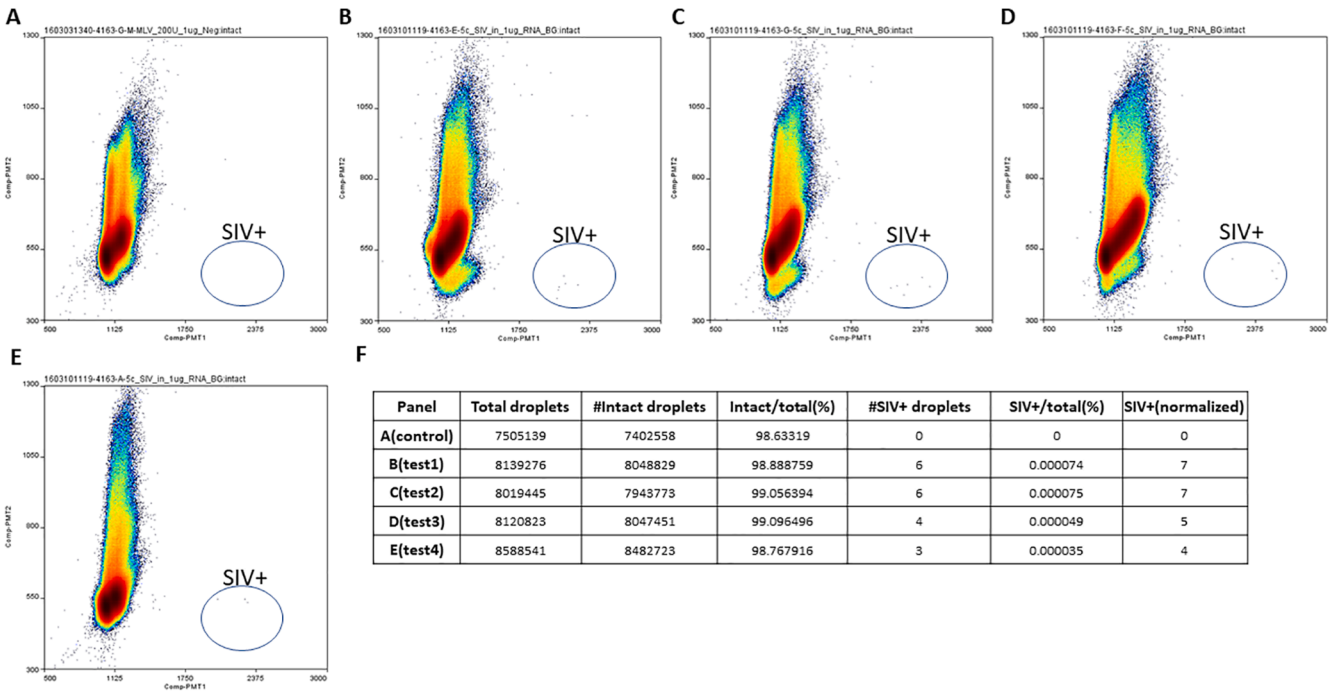

Panel	Total droplets	#Intact droplets	Intact/total(%)	#SIV+ droplets	SIV+/total(%)	SIV+(normalized)
A(control)	7505139	7402558	98.63319	0	0	0
B(test1)	8139276	8048829	98.888759	6	0.000074	7
C(test2)	8019445	7943773	99.056394	6	0.000075	7
D(test3)	8120823	8047451	99.096496	4	0.000049	5
E(test4)	8588541	8482723	98.767916	3	0.000035	4

Fig. 6. Low level SIV RNA signal detection on the Raindance platform using the SIV RT-ddPCR assay. (A) A negative control sample which contains 1 μg background RNA extracted from the peripheral blood mononuclear cells (PBMC) from a naïve (i.e. uninfected) animal. (B-E) each corresponds to an average of 5 copies of SIV RNA standard spiked in 1 μg background RNA extracted from the PBMC from the same naïve animal as in (A). "SIV+" indicates SIV positive droplets. (F) Quantitation and statistics data corresponding to (A-E). The normalized SIV + values were calculated as described in [20]. The average SIV + value for (B-E) was 6, and the coefficient of variation (CV) was 26.1%. Note that at the 5-copy target input level, the exact copies of the target templates that are present in the reactions follow a Poisson distribution, due to the stochastic limitations inherent in target sequence distribution in the volume of sample aliquots taken for testing.

potential contamination. In addition, due to the Raindance ddPCR platform's high capacity for DNA input, there is little or no need for the labor-intensive sample dilution and repeat testing steps. As the amount of total nucleic acid that can be analyzed in each reaction (without introducing significant inhibition) is an important decisive factor of the overall assay sensitivity, many qPCR methods (including our qPCR-based tissue DNA analysis method described above [55,56]) and digital PCR platforms with lower sample input capacity in each reaction often use multiple replicates to sidestep the per reaction sample input limit. For example, to analyze 10 million mammalian cell equivalent DNA for the presence of low-level viral signals, a ddPCR platform that allows an upper limit of 1 μg DNA per reaction would require 66 reactions, while the Raindance ddPCR platform used in the current protocol can handle the same quantity of input sample with triplicate reactions without reaction inhibition. In addition, in the current protocol, we have introduced a higher volume (i.e. 5 mL) processing option during quantitative nucleic acid recovery from tissue samples, taking advantage of commercially available 5 mL microfuge tubes that can stand up to 25,000 xg centrifugation forces, to increase nucleic acid yield. This is important as the current protocol is intended to enable routine analysis of 3 million or more cell equivalent of tissue DNA (per reaction) to allow detection and quantification of low level viral nucleic acids as shown in Fig. 5. Overall, through a combination of higher sample processing throughput at the nucleic acid quantitative recovery step, and significantly increased nucleic acid input at the assay step, the current protocol can potentially benefit HIV cure research (e.g. to allow assessing and comparing the efficacy of treatment regimens, and differentiating between suppressed low viral state and eradication) and other research areas. Additional application examples were described [20,21] illustrating the utility of the assays and protocol in analyzing SIV in nucleic acids extracted from primary tissues from SIV-infected Rhesus macaques that were chronically suppressed with cART (i.e. with extremely low viral load). In addition, the accompanying review article [54] provides a detailed discussion of the factors that contribute to achieving optimal detection sensitivity on this platform.

One main factor that contributes to ddPCR experiment success is droplet integrity. Issues can manifest themselves as non-uniform droplet generation, poor droplet stability (post-generation), or coalescence of drops during thermal cycling. Compromised emulsion quality or droplet stability can lead to artifacts that can interfere with droplet clustering and gating, in that the artifacts can fall within the target gates and adversely affect the droplet counts, often making it difficult to gate clusters. At the droplet generation stage, particulate debris in reagents or nucleic acid samples can destabilize the emulsion. This can be resolved by filtering water, Tris or other reagents used for resuspending or preparing primers, probes, nucleic acids and sample stocks, or by purifying the nucleic acid samples using filter-based kits. Another issue that can contribute to poor droplet stability is when unsheared or improperly sheared DNA (i.e. DNA that is too long) is overloaded into the reaction. In this case, either the amount of unsheared DNA should be reduced in the reaction, or the DNA sample can be re-sheared or renebulized to the appropriate length as determined using an Agilent Bioanalyzer or agarose gel. At the thermal cycling step, if the heated lid is not adequately adjusted (either due to the heated lid not functioning, or the lid not properly tightened) or the PCR tube caps are sealed improperly, evaporation and condensation can occur, which can lead to a decrease in droplet stability as well. In addition, static build-up on plasticware (including PCR tubes), equipment and synthetic lab clothing can significantly compromise the droplets as well. This is especially so when the air is extremely dry such as under aggressive air conditioning or low external temperature conditions. Increasing the humidity of the lab space with a humidifier, using an antistatic mat below the thermal cycler and in the reaction set-up area, storing PCR tubes in anti-static bags, and using non-polyester lab coats and nitrile gloves can help discharge static and resolve static-related droplet stability issues. Finally, PCR master mix recipes may contain or lack additives that can influence droplet

stability. This issue can be resolved by testing reactions by omitting or adding additives (such as magnesium chloride and tetramethylammonium chloride, among others) for in-house PCR master mixes. However, due to the proprietary nature of most commercially available master mixes, troubleshooting the droplet integrity/stability issue in commercial master mixes can be challenging.

False positives and false negatives are two other factors that can lead to inaccurate ddPCR quantitation. Due to its high sensitivity, the Raindance ddPCR system can often reveal the presence of reagent or workspace contamination that may evade detection by less sensitive methods (including qPCR). Therefore, it is imperative that reagents free of contaminants are used in ddPCR reactions, and the pre-PCR and post-PCR workspaces are separated to reduce the risk of airborne amplicons from contaminating reagents. The reagent contamination issue has been highlighted by recent reports demonstrating the occurrence of such contamination during SARS-CoV-2 diagnostics and the delayed laboratory response to COVID-19 caused by such molecular diagnostic contamination [60,61]. In addition to contamination, poorly designed assays and detection of pseudogenes can also lead to false positives (including unexpected clusters), with the pseudogene signals often scaling with nucleic acid loading into the reaction. The issue can be resolved by using amplicons designed for unique segments of the genome so that pseudogenes are not detected and do not falsely contribute to positive droplet signals.

False negatives (i.e. lower than expected positive counts) are often caused by compromised nucleic acid template quality, assuming the assay has been properly validated and optimized. During sample preparation and DNA shearing, a portion of the DNA will become unamplifiable from breaks within target regions. In addition, upstream storage and treatment of the sample can also influence the proportion of the DNA that is amplifiable. When suspected false negatives or underquantification occurs, evaluating an intact control DNA sample (such as a synthetic template) of a known quantity can help ensure that amplification performance of the assay under the ddPCR condition is accurate. In addition, target template spikes can help monitor the effect of sample storage, processing, DNA preparation and shearing on the amplifiable fraction.

Probe quality and fluorescence influence the location of gates that are used in defining the positive cluster gates. Therefore, reduced quality or batch-to-batch variation in a probe may necessitate cluster gating adjustments during data analysis. The quality of probes can be evaluated through the use of qPCR. Most qPCR instrument software is equipped with a function to plot the amplification curve without background subtraction (i.e. the raw fluorescent units). This option can be used to calculate the fluorescence gain, which is the difference between the fluorescence intensity at the endpoint and that at the first cycle. In general, similar fluorescence gain values between test lots and reference lots will lead to comparable assay performance in ddPCR, while large differences in fluorescence gain values will lead to significant cluster shifts in the ddPCR plotting space. As a rule of thumb, a $\geq$ 10% decrease in the fluorescence gain in a test probe lot often correlates with reduced ddPCR performance, and a $\geq$ 30% decrease in fluorescence gain often leads to ddPCR reaction failure.

6. Conclusion

Viral nucleic acid detection and quantitation by PCR is the method of choice for early diagnosis of infectious diseases such as COVID-19 and HIV-1. Assay sensitivity often determines the diagnosis outcome, and in many cases, how early the infection can be discovered and contained, and how early the disease can be treated. The upstream method used to extract nucleic acids, and the platform on which the assays are performed also contribute significantly to the overall assay performance. In the current report, protocols are described to allow quantitative recovery of DNA and RNA from tissue samples, and ultrasensitive ddPCR assays are combined with the Raindance ddPCR platform to enable sensitive detection and quantification of SIV viral signals. Similar protocols can be adapted for other applications where sensitive detection of nucleic acids is required especially when a large quantity of background nucleic acids is present, or when inhibitors are present. We anticipate that this protocol will enable sensitive viral detection in animal tissues/cells and development of similar protocols in related fields.

CRediT authorship contribution statement

Samuel Long: Methodology, Investigation, Validation, Conceptualization, Project administration, Resources, Writing - review & editing. **Brian Berkemeier:** Methodology, Investigation, Validation.

Declaration of competing interest

The authors declare no known competing financial interests or personal relationships that could have appeared to influence the work reported in this manuscript.

Acknowledgements

This project has been funded with Federal funds from the National Cancer Institute, National Institutes of Health, under contract numbers HHSN261200800001E and 75N91019D00024. The content of this publication does not necessarily reflect the views or policies of the Department of Health and Human Services, nor does mention of trade names, commercial products, or organizations imply endorsement by the US Government. The authors would like to acknowledge Dr. Robert Gorelick for valuable comments on the manuscript. Rhesus macaque tissue specimens were graciously provided by Dr. Paul Johnson (Emory University).

Ethics approval statement

Rhesus macaques (Macaca mulatta) were housed and cared for in compliance with American Association for Accreditation of Laboratory Animal Care (AAALAC) guidelines in AAALAC-accredited facilities, and all animal procedures were performed in accordance with protocols approved by the Institutional Animal Care and Use Committee of the National Cancer Institute under the standards of the NIH guide for the Care and Use of Laboratory Animals, and the Emory University Institutional Animal Care and Use Committee, respectively.

References

[1] V.M. Corman, O. Landt, M. Kaiser, R. Molenkamp, A. Meijer, D.K. Chu, Detection of 2019 novel coronavirus (2019-nCoV) by real-time RT-PCR, Euro Surveill. 25 (2020) 2000045.
[2] Coronavirus Disease Available from: COVID-19 2019 2020 https://www.cdc.gov/coronavirus/2019-ncov/lab/rt-pcr-panel-primer-probes.html.
[3] B.B. Policicchio, E.F. Cardozo, P. Sette, C. Xu, G. Haret-Richter, T. Dunsmore, C. Apetrei, I. Pandrea, R.M. Ribeiro, Dynamics of simian immunodeficiency virus two-long-terminal-repeat circles in the presence and absence of CD8+ cells, J. Virol. 92 (2018) e02100–e2117.
[4] C.H. Birkenheuer, C.G. Danko, J.D. Baines, Herpes Simplex virus 1 dramatically alters loading and positioning of RNA polymerase II on host genes early in infection, J. Virol. 92 (2018) e02184–e2217.
[5] K.E. Sherman, S.D. Rouster, L.X. Kong, M.T. Aliota, J.T. Blackard, G.E. Dean, Zika virus replication and cytopathic effects in liver cells, PLoS One. 14(2019): e0214016.
[6] L.L. Jagodzinski, M.M. Manak, H.R. Hack, Y. Liu, S.A. Peel, Performance evaluation of a laboratory developed PCR test for quantitation of HIV-2 viral RNA, PLoS One. 15(2020):e0229424.
[7] F. Calascibetta, L. Micci, D. Carnathan, B. Lawson, T.H. Vanderford, S.E. Bosinger, K. Easley, A. Chahroudi, J. Mackel, B.F. Keele, S. Long, J. Lifson, M. Paiardini, G. Silvestri, Antiretroviral therapy in simian immunodeficiency virus-infected sooty mangabeys: Implications for AIDS pathogenesis, J Virol. 90 (2016) 7541–7551.
[8] A.Whitmill, S. Kim, V. Rojas, F. Gulraiz, K. Afreen, M. Jain, M. Singh, I.W. Park, Signature molecules expressed differentially in a liver disease stage-specific manner by HIV-1 and HCV co-infection, PLoS One. 13(2018):e0202524.

[9] S. Palmer S, A.P. Wiegand, F. Maldarelli, H. Bazmi, J.M. Mican, M. Polis, R.L. Dewar, A. Planta, S. Liu, J.A. Metcalf, J.W. Mellors, J.M. Coffin, New real-time reverse transcriptase-initiated PCR assay with single-copy sensitivity for human immunodeficiency virus type 1 RNA in plasma, J. Clin. Microbiol. 41 (2013): 4531-4536.
[10] J.P. Williams, J. Hurst, W. Stöhr, N. Robinson, H. Brown, M. Fisher, S. Kinloch, D. Cooper, M. Schechter, G. Tambussi, S. Fidler, M. Carrington, A. Babiker, J. Weber, K.K. Koelsch, A.D. Kelleher, R.E. Phillips, J. Frater, SPARTACTrial investigators, HIV-1 DNA predicts disease progression and post-treatment virological control, Elife. 3 (2014), e03821.
[11] A.S. Whale, J.F. Huggett, S. Tzonev, Fundamentals of multiplexing with digital PCR, Biomol Detect Quantif. 10 (2016) 15–23, https://doi.org/10.1016/j.bdq.2016.05.002.
[12] dMIQE Group, J.F. Huggett, The Digital MIQE Guidelines Update: Minimum Information for Publication of Quantitative Digital PCR Experiments for 2020. Clin Chem. 66(2020):1012-1029.
[13] J.F. Huggett, C.A. Foy, V. Benes, K. Emslie, J.A. Garson, R. Haynes, J. Hellemans, M. Kubista, R.D. Mueller, T. Nolan, M.W. Pfaffl, G.L. Shipley, J. Vandesompele, C. T. Wittwer, S.A. Bustin, The digital MIQE guidelines: Minimum information for publication of quantitative digital PCR experiments, Clin Chem. 59 (2013) 892–902.
[14] M.R. Openshaw, A.A. Mohamed, B. Ottolini, D. Fernandez-Garcia, C.J. Richards, K. Page, D.S. Guttery, A.L. Thomas, J.A. Shaw, Longitudinal monitoring of circulating tumour DNA improves prognostication and relapse detection in gastroesophageal adenocarcinoma, Br. J. Cancer. 123 (2020) 1271–1279.
[15] E. Zulato, I. Attili, A. Pavan, G. Nardo, P. Del Bianco, A. Boscolo Bragadin, M. Verza, L. Pasqualini, G. Pasello, M. Fassan, F. Calabrese, V. Guarneri, A. Amadori, P. Conte, S. Indraccolo, L. Bonanno, Early assessment of KRAS mutation in cfDNA correlates with risk of progression and death in advanced non-small-cell lung cancer, Br J Cancer. 123(2020):81-91.
[16] M. Del Re, P. Bordi, E. Rofi, G. Restante, S. Valleggi, R. Minari, S. Crucitta, E. Arrigoni, A. Chella, R. Morganti, M. Tiseo, I. Petrini, R. Danesi, The amount of activating EGFR mutations in circulating cell-free DNA is a marker to monitor osimertinib response, Br. J. Cancer. 119 (2018) 1252–1258.
[17] M. Brait, E. Izumchenko, L.T. Kagohara, S. Long, P.T. Wysocki, B. Faherty, E. J. Fertig, T.O. Khor, E. Bruckheimer, G. Baia, D. Ciznadija, I. Sloma, I. Ben-Zvi, K. Paz, D. Sidransky, Comparative mutational landscape analysis of patient-derived tumour xenografts, Br. J. Cancer 116 (2017) 515–523.
[18] L. Lindner, P. Cayrou, T.W. Rosahl, H.E. Zhou, M.C. Birling, Y. Herault, G. Pavlovic, Droplet digital PCR or quantitative PCR for in-depth genomic and functional validation of genetically altered rodents, Methods (2021), https://doi.org/10.1016/j.ymeth.2021.04.001.
[19] S.F. Rosa, F. Gatto, A. Angers-Loustau, M. Petrillo, J. Kreysa, M. Querci, Development and applicability of a ready-to-use PCR system for GMO screening, Food Chem. 201 (2016) 110–119.
[20] S. Long, B. Berkemeier, Maximizing viral detection with SIV droplet digital PCR (ddPCR) assays, PLoS One. 15(2020a):e0233085. doi: 10.1371/journal.pone.0233085.
[21] S. Long, B. Berkemeier, Development and optimization of a simian immunodeficiency virus (SIV) droplet digital PCR (ddPCR) assay, PLoS One. 15 (2020b):e0240447. doi: 10.1371/journal.pone.0240447.
[22] J.R. Pieknik, A.S. Bertke, P.R. Krause PR, Herpes Simplex Virus 2 in Autonomic Ganglia: Evidence for Spontaneous Reactivation, J Virol. 93(2019):e00227-19.
[23] C. Alteri, V. Cento, M. Antonello, L. Colagrossi, M. Merli, N. Ughi, S. Renica, E. Matarazzo, F. Di Ruscio, L. Tartaglione, J. Colombo, C. Grimaldi, S. Carta, A. Nava, V. Costabile, C. Baiguera, D. Campisi, D. Fanti, C. Vismara, R. Fumagalli, F. Scaglione, O.M. Epis, M. Puoti, C.F. Perno, Detection and quantification of SARS-CoV-2 by droplet digital PCR in real-time PCR negative nasopharyngeal swabs from suspected COVID-19 patients. PLoS One. 15(2020):e0236311.
[24] L. Falzone, N. Musso, G. Gattuso, D. Bongiorno, C.I. Palermo, G. Scalia, M. Libra, S. Stefani, Sensitivity assessment of droplet digital PCR for SARS-CoV-2 detection, Int. J. Mol. Med. 46 (2020) 957–964.
[25] D. Veyer, S. Kernéis, G. Poulet, M. Wack, N. Robillard, V. Taly, A.S. L'Honneur, F. Rozenberg, P. Laurent-Puig, L. Bélec, J. Hadjadj, B. Terrier, H. Péré. Highly sensitive quantification of plasma SARS-CoV-2 RNA shelds light on its potential clinical value. Clin Infect Dis. 2020 Aug 17:ciaa1196.
[26] L. Gibellini, S. Pecorini, S. De Biasi, M. Pinti, E. Bianchini, A. De Gaetano, M. Digaetano, R. Pullano, D. Lo Tartaro, A. Iannone, C. Mussini, A. Cossarizza, M. Nasi, Exploring viral reservoir: The combining approach of cell sorting and droplet digital PCR, Methods 134–135 (2018) 98–105.
[27] S. Long, B. Berkemeier, Development of a reverse transcription droplet digital PCR (RT-ddPCR) assay for sensitive detection of simian immunodeficiency virus (SIV), Virology J. (2021), https://doi.org/10.1186/s12985-021-01503-5.
[28] S. Falak, R. Macdonald, E.J. Busby, D.M. O'Sullivan, M. Milavec, A. Plauth, M. Kammel, H. Zeichhardt, H.P. Grunert, A. Kummrow, J.F. Huggett JF, An assessment of the reproducibility of reverse transcription digital PCR quantification of HIV-1, Methods (2021), https://doi.org/10.1016/j.ymeth.2021.03.006.
[29] M. Milavec, J. Pavšič, A.B. Košir, G.M. Jones, D.M. O'Sullivan, A.S. Devonshire, F. Van Heuverswyn, M. Karczmarczyk, J. Neeb, A. Plauth, P. Corbisier, H. Schimmel, A. Kummrow, J. Neukammer, C.A. Foy, M. Kammel, H.P. Grunert, H. Zeichhardt, J.F. Huggett, The performance of human cytomegalovirus digital PCR reference measurement procedure in seven external quality assessment schemes over four years, Methods (2021), https://doi.org/10.1016/j.ymeth.2021.03.016.
[30] L. Piermatteo, R. Scutari, R. Chirichiello, M. Alkhatib, V. Malagnino, A. Bertoli, N. Iapadre, M. Ciotti, L. Sarmati, M. Andreoni, F. Ceccherini-Silberstein, R. Salpini, V. Svicher, Droplet digital PCR assay as an innovative and promising highly sensitive assay to unveil residual and cryptic HBV replication in peripheral compartment, Methods (2021), https://doi.org/10.1016/j.ymeth.2021.05.011.
[31] W. van Snippenberg, D. Gleerup, S. Rutsaert, L. Vandekerckhove, W. De Spiegelaere, W. Trypsteen, Triplex digital PCR assays for the quantification of intact proviral 2 HIV-1 DNA, Methods (2021), https://doi.org/10.1016/j.ymeth.2021.05.006.
[32] S. Telwatte, H.A. Martin, R. Marczak, P. Fozouni, A. Vallejo-Gracia, G.R. Kumar, V. Murray, S. Lee, M. Ott, J.K. Wong, S.A. Yukl, Novel RT-ddPCR assays for measuring the levels of subgenomic and genomic SARS-CoV-2 transcripts, Methods (2021), https://doi.org/10.1016/j.ymeth.2021.04.011.
[33] S. Telwatte, N. Kumar, A. Vallejo-Gracia, G.R. Kumar, C.M. Lu, M. Ott, J.K. Wong, S.A. Yukl, Novel RT-ddPCR assays for simultaneous quantification of multiple noncoding and coding regions of SARS-CoV-2 RNA, J Virol Methods (2021), https://doi.org/10.1016/j.jviromet.2021.114115.
[34] K.K. Dickinson, L.C. Hammond, C.M. Karner, N.D. Hastie, T.J. Carroll, P. Goodyer, Molecular determinants of WNT9b responsiveness in nephron progenitor cells, PLoS ONE 14 (2019), e0215139.
[35] L. Lindner, P. Cayrou, S. Jacquot, M.-C. Birling, Y. Herault, G. Pavlovic, Reliable and robust droplet digital PCR (ddPCR) and RT-ddPCR protocols for mouse studies, Methods (2020), https://doi.org/10.1016/j.ymeth.2020.07.004.
[36] J. Monico, B. Miller, L. Rezeanu, W. May, D.C. Sullivan, Fibroblast growth factor receptor 1 amplification in laryngeal squamous cell carcinoma, PLoS ONE 13 (2018), e0186185.
[37] S. Weaver, S. Dube, A. Mir, J. Qin, G. Sun, R. Ramakrishnan, R.C. Jones, K.J. Livak, Taking qPCR to a higher level: Analysis of CNV reveals the power of high throughput qPCR to enhance quantitative resolution, Methods 50 (2010) 271–276.
[38] S. Hellwig, D.A. Nix, K.M. Gligorich, J.M. O'Shea, A. Thomas, C.L. Fuertes, P. J. Bhetariya, G.T. Marth, M.P. Bronner, H.R. Underhill, Automated size selection for short cell-free DNA fragments enriches for circulating tumor DNA and improves error correction during next generation sequencing, PLoS ONE 13 (2018), e0197333.
[39] S. Rutsaert, K. Bosman, W. Trypsteen, M. Nijhuis, L. Vandekerckhove, Digital PCR as a tool to measure HIV persistence, Retrovirology. 15(2018):16. doi: 10.1186/s12977-018-0399-0.
[40] L. Dong, J. Zhou, C. Niu, Q. Wang, Y. Pan, S. Sheng, X. Wang, Y. Zhang, J. Yang, M. Liu, Y. Zhao, X. Zhang, T. Zhu, T. Peng, J. Xie, Y. Gao, D. Wang, X. Dai, X. Fang, Highly accurate and sensitive diagnostic detection of SARS-CoV-2 by digital PCR, Talanta 27 (2020), 121726, https://doi.org/10.1016/j.talanta.2020.121726.
[41] T. Suo, X. Liu, J. Feng, M. Guo, W. Hu, D. Guo, H. Ullah, Y. Yang, Q. Zhang, X. Wang, M. Sajid, Z. Huang, L. Deng, T. Chen, F. Liu, K. Xu, Y. Liu, Q. Zhang, Y. Liu, Y. Xiong, G. Chen, K. Lan, Y. Chen, ddPCR: A more accurate tool for SARS-CoV-2 detection in low viral load specimens, Emerg. Microbes. Infect. 9 (2020) 1259–1268.
[42] K. Cassinari, E. Alessandri-Gradt, P. Chambon, F. Charbonnier, S. Gracias, L Beaussire., K. Alexandre, N. Sarafan-Vasseur, C. Houdayer, M. Etienne, F. Caron, J. C. Plantier, T. Frebourg, Assessment of multiplex digital droplet RT-PCR as a diagnostic tool for SARS-CoV-2 detection in nasopharyngeal swabs and saliva samples. Clin Chem, 2020 Dec 17;hvaa323. doi: 10.1093/clinchem/hvaa323.
[43] R.H. Sedlak, L. Cook, A. Cheng, A. Magaret, K.R. Jerome, Clinical utility of droplet digital PCR for human cytomegalovirus, J. Clin. Microbiol.. 52 (2014) 2844–2848.
[44] T. Demeke, D. Dobnik, Critical assessment of digital PCR for the detection and quantification of genetically modified organisms, Anal. Bioanal. Chem. 410 (2018) 4039–4050.
[45] L.J. Henderson, L.B. Reoma, J.A. Kovacs, A. Nath, Advances toward Curing HIV-1 Infection in Tissue Reservoirs, J. Virol. 94 (2020) e00375–e419.
[46] A. Shen, M.C. Zink, J.L. Mankowski, K. Chadwick, J.B. Margolick, L.M. Carruth, M. Li, J.E. Clements, R.F. Siliciano, Resting CD4+ T lymphocytes but not thymocytes provide a latent viral reservoir in a simian immunodeficiency virus-Macaca nemestrina model of human immunodeficiency virus type 1-infected patients on highly active antiretroviral therapy, J. Virol. 77 (2003) 4938–4949.
[47] J.B. Dinoso, S.A. Rabi, J.N. Blankson, L. Gama, J.L. Mankowski, R.F. Siliciano, M. C. Zink, J.E. Clements, A simian immunodeficiency virus-infected macaque model to study viral reservoirs that persist during highly active antiretroviral therapy, J. Virol. 83 (2009) 9247–9257.
[48] M.E. Moreno-Fernandez, P. Presicce, C.A. Chougnet, Homeostasis and function of regulatory T cells in HIV/SIV infection, J Virol. 86 (2012) 10262–10269.
[49] J.B. Whitney, A.L. Hill, S. Sanisetty, P. Penaloza-MacMaster, J. Liu, M. Shetty, L. Parenteau, C. Cabral, J. Shields, S. Blackmore, J.Y. Smith, A.L. Brinkman, L. E. Peter, S.I. Mathew, K.M. Smith, E.N. Borducchi, D.I. Rosenbloom, M.G. Lewis, J. Hattersley, B. Li, J. Hesselgesser, R. Geleziunas, M.L. Robb, J.H. Kim, N. L. Michael, D.H. Barouch, Rapid seeding of the viral reservoir prior to SIV viraemia in rhesus monkeys, Nature 512 (2014) 74–77.
[50] E.N. Borducchi, C. Cabral, K.E. Stephenson, J. Liu, P. Abbink, D. Ng'ang'a, J. P. Nkolola, A.L. Brinkman, L. Peter, B.C. Lee, J. Jimenez, D. Jetton, J. Mondesir, S. Mojta, A. Chandrashekar, K. Molloy, G. Alter, J.M. Gerold, A.L. Hill, M.G. Lewis, M.G. Pau, H. Schuitemaker, J. Hesselgesser, R. Geleziunas, J.H. Kim, M.L. Robb, N. L. Michael, D.H. Barouch, Ad26/MVA therapeutic vaccination with TLR7 stimulation in SIV-infected rhesus monkeys, Nature 540 (2016) 284–287.
[51] E. Krakoff, R.B. Gagne, S. VandeWoude, S. Carver, Variation in Intra-individual lentiviral evolution rates: A systematic review of human nonhuman primate, and felid species, J. Virol. 93 (2019) e00538–e619.
[52] S. Long, C.M. Fennessey, L. Newman, C. Reid, S.P. O'Brien, Y. Li, G.Q. Del Prete, J. D. Lifson, R.J. Gorelick, B.F. Keele, Evaluating the intactness of persistent viral genomes in simian immunodeficiency virus-infected rhesus macaques after

initiating antiretroviral therapy within one year of infection, J. Virol. 94 (2019) e01308–e1319.
[53] A.O. Pasternak, M.L. Grijsen, F.W. Wit, M. Bakker, S. Jurriaans, J.M. Prins, B. Berkhout, Cell-associated HIV-1 RNA predicts viral rebound and disease progression after discontinuation of temporary early ART, JCI Insight. 5(2020): e134196.
[54] S. Long, In pursuit of sensitivity: lessons learned from viral nucleic acid detection and quantification on the Raindance ddPCR platform, Methods S1046–2023(21) 00100-6 (2021), https://doi.org/10.1016/j.ymeth.2021.04.008.
[55] S.G. Hansen, E.E. Marshall, D. Malouli, A.B. Ventura, C.M. Hughes, E. Ainslie, J.C. Ford, D. Morrow, R.M. Gilbride, J.Y. Bae, A.W. Legasse, K. Oswald, R. Shoemaker, B. Berkemeier, W.J. Bosche, M. Hull, J. Womack, J. Shao, P.T. Edlefsen, J.S. Reed, B.J. Burwitz, J.B. Sacha, M.K. Axthelm, K. Früh, J.D. Lifson, L.J. Picker, A live-attenuated RhCMV/SIV vaccine shows long-term efficacy against heterologous SIV challenge, Sci Transl Med. 11(2019):eaaw2607.
[56] J. Liu, K. Ghneim, D. Sok, W.J. Bosche, Y. Li, E. Chipriano, B. Berkemeier, K. Oswald, E. Borducchi, C. Cabral, L. Peter, A. Brinkman, M. Shetty, J. Jimenez, J. Mondesir, B. Lee, P. Giglio, A. Chandrashekar, P. Abbink, A. Colantonio, C. Gittens, C. Baker, W. Wagner, M.G. Lewis, W. Li, R.P. Sekaly, J.D. Lifson, D. R. Burton, D.H. Barouch, Antibody-mediated protection against SHIV challenge includes systemic clearance of distal virus, Science 353 (2016) 1045–1049.
[57] P.T.K. Lin, D.M. Brown, Synthesis of oligodeoxyribonucleotides containing degenerate bases and their use as primers in the polymerase chain reaction, Nucleic Acids Res. 20 (1992) 5149–5152.
[58] M.C. Strain, S.M. Lada, T. Luong, S.E. Rought, S. Gianella, H. Terry, C.A. Spina, C. H. Woelket, D.D. Richman, Highly precise measurement of HIV DNA by droplet digital PCR, PLoS ONE 8 (2013), e55943.
[59] Z. Nie, M. Seo, S. Xu, P.C. Lewis, M. Mok, E. Kumacheva, G.M. Whitesides, P. Garstecki, H.A. Stone, Emulsification in a microfluidic flow-focusing device: effect of the viscosities of the liquids, Microfluid. Nanofluid. 5 (2008) 585–594.
[60] K. Wernike, M. Keller, F.J. Conraths, T.C. Mettenleiter, M.H. Groschup, M. Beer, Pitfalls in SARS-CovV2 PCR diagnostics, Transbound. Emerg. Dis. (2020), https://doi.org/10.1111/tbed.13684.
[61] R. Mogling, A. Meijer, N. Berginc, S. Bruisten, R. Charrel, B. Coutard, I. Eckerle, V. Enouf, O. Hungnes, G. Korukluoglu, T. Kossyvakis, A. Mentis, R. Molenkamp, S. Muradrasoli, A. Papa, F. Pigny, L. Thirion, S. van der Werf, C. Reusken, Delayed laboratory response to covid-19 caused by molecular diagnostic contamination, Emerg. Infect. Dis. 26 (2020) 1944–1946.